

63-3-2

ASD-TDR-62-323

401 811

CATALOGED BY ASTIA
AS AD No. 401811

ANELASTIC BEHAVIOR OF TANTALUM AND COLUMBIUM

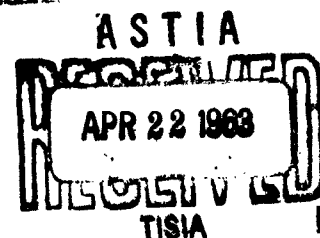
TECHNICAL DOCUMENTARY REPORT NO. ASD-TDR-62-323

February 1963

DIRECTORATE OF MATERIALS AND PROCESSES
AERONAUTICAL SYSTEMS DIVISION
AIR FORCE SYSTEMS COMMAND
WRIGHT-PATTERSON AIR FORCE BASE, OHIO

Project No. 7351, Task No. 735106

(Prepared under Contract No. AF 33(616)-7235
by General Dynamics/Pomona, Pomona, Cal.
R. J. Sneed, E. L. Fink, M. C. Abrams, authors.)



NOTICES

When Government drawings, specifications, or other data are used for any purpose other than in connection with a definitely related Government procurement operation, the United States Government thereby incurs no responsibility nor any obligation whatsoever; and the fact that the Government may have formulated, furnished, or in any way supplied the said drawings, specifications, or other data, is not to be regarded by implication or otherwise as in any manner licensing the holder or any other person or corporation, or conveying any rights or permission to manufacture, use, or sell any patented invention that may in any way be related thereto.

Qualified requesters may obtain copies of this report from the Armed Services Technical Information Agency, (ASTIA), Arlington Hall Station, Arlington 12, Virginia.

This report has been released to the Office of Technical Services, U.S. Department of Commerce, Washington 25, D.C., in stock quantities for sale to the general public.

Copies of this report should not be returned to the Aeronautical Systems Division unless return is required by security considerations, contractual obligations, or notice on a specific document.

Aeronautical Systems Division, Dir/Materials and Processes, Metals and Ceramics Lab., Wright-Patterson AFB, Ohio.
Rpt Mr ASD-TDR-62-323. ANELASTIC BEHAVIOR OF TANTALUM AND COLUMBIUM. Final report, Feb 63, 121 p. Incl illus., tables, and 49 refs.

Unclassified report

A theoretical model is developed based on dislocation-interstitial interaction during stress application, which describes the yield delay behavior in bcc metals. Reorientation of interstitial impurities apparently controls both the pre-yield microstrain rate and the time to yield. The model

(over)

is supported for Ta and Nb by the results of yield delay experiments over a temperature range from -97°F to 400°F. Activation energies of the yield delay process indicate that hydrogen has a controlling effect, with other interstitials contributing.

The model is further substantiated by x-ray diffractometry which demonstrates the occurrence of anelastic lattice strains during load application and their consequent recovery.

A brief resume is given on the initial efforts of a high temperature study on the anelasticity in tantalum and columbium.

1. Yield delay, columbium and tantalum
2. X-ray diffractometry during yield delay, Ta and Nb
3. Preferential interstitial diffusion, Ta and Nb

I. Project 7351
Task 735106

II. Contract AF 33(616)-7235

III. General Dynamics/Pomona, Pomona, California

IV. R. J. Speed, E. L. Fink, M. C. Abrams

Aeronautical Systems Division, Dir/Materials and Processes, Metals and Ceramics Lab., Wright-Patterson AFB, Ohio.
Rpt Mr ASD-TDR-62-323. ANELASTIC BEHAVIOR OF TANTALUM AND COLUMBIUM. Final report, Feb 63, 121 p. Incl illus., tables, and 49 refs.

Unclassified report

A theoretical model is developed based on dislocation-interstitial interaction during stress application, which describes the yield delay behavior in bcc metals. Reorientation of interstitial impurities apparently controls both the pre-yield microstrain rate and the time to yield. The model

(over)

is supported for Ta and Nb by the results of yield delay experiments over a temperature range from -97°F to 400°F. Activation energies of the yield delay process indicate that hydrogen has a controlling effect, with other interstitials contributing.

The model is further substantiated by x-ray diffractometry which demonstrates the occurrence of anelastic lattice strains during load application and their consequent recovery.

A brief resume is given on the initial efforts of a high temperature study on the anelasticity in tantalum and columbium.

1. Yield delay, columbium and tantalum
2. X-ray diffractometry during yield delay, Ta and Nb
3. Preferential interstitial diffusion, Ta and Nb

I. Project 7351
Task 735106

II. Contract AF 33(616)-7235

III. General Dynamics/Pomona, Pomona, California

IV. R. J. Speed, E. L. Fink, M. C. Abrams

V. Avail fr ODS

VI. In ASTIA collection

FOREWORD

This report was prepared by the Physics and Infrared Section of General Dynamics/Pomona under Contract No. AF 33(616)-7235, Project No. 7351, "Metallic Materials, Task No. 735106, "Behavior of Metals". The work was administered by the Directorate of Materials and Processes, Deputy for Technology, Aeronautical Systems Division, Wright-Patterson Air Force Base, Ohio. Mr. B. A. Wilcox and, subsequently Mr. G. W. King acted as project engineers.

This report covers work performed during the period of March 1960 to October 1961.

The authors wish to express their appreciation to the personnel of the General Dynamics/Pomona Structural Test Laboratory, in particular Messrs. J. E. Cole and C. E. Setterland, for their outstanding contributions to all phases of the experimental work under this contract.

The valuable assistance of Dr. Alex Baird and the Department of Geology of the Pomona College in obtaining x-ray diffractometer data are gratefully acknowledged.

A special note of thanks must go to Dr. Hum of the Stauffer Metals Company who helped us over a critical period in this contract by offering his talents and facilities for the high vacuum, high temperature heat treatment of all experimental specimens.

The personnel of the Materials and Processing Section of General Dynamics deserve credit for their competent contributions in the preparation and metallography of the experimental materials.

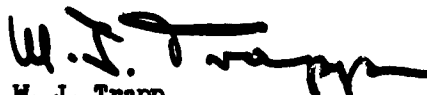
ABSTRACT

A theoretical model is developed based on dislocation-interstitial interaction during stress application, which describes the anelastic behavior of bcc metals particularly during yield delay. It is shown that the re-orientation of interstitial impurities apparently controls both the pre-yield microstrain rate and the time to yield. The model is supported for tantalum and columbium by the results of yield delay experiments over a temperature range from -97°F to 400°F . Activation energies of the yield delay process calculated both from microstrain rate data and time to yield information indicate that hydrogen diffusion has a controlling effect, with other interstitials contributing to the effective activation energies at the higher temperatures. Temperature insensitive stress effects are noted.

The model is further substantiated by x-ray diffractometry which demonstrates the occurrence of anelastic lattice strains during load application and their consequent recovery.

A brief resume is given on the initial efforts of a high temperature study on the anelasticity in tantalum and columbium. This study is aimed at exploring anelastic behavior up to 3000°F .

This technical documentary report has been reviewed and is approved.



W. J. Trapp
Chief, Strength and Dynamics Branch
Metals and Ceramics Laboratory
Directorate of Materials and Processes

TABLE OF CONTENTS

INTRODUCTION	1
THEORETICAL BACKGROUND	5
DISLOCATION MODEL	5
INTERSTITIAL DIFFUSION MODEL	9
PROPOSED MODEL, DISLOCATION - INTERSTITIAL INTERACTION	10
TENSILE EXPERIMENTS	21
DISCUSSION	21
EXPERIMENTAL TECHNIQUES	22
Specimens	22
Equipment	28
Experimental Procedure	31
RESULTS AND INTERPRETATIONS	37
X-RAY DIFFRACTION MEASUREMENTS OF MICROSTRAIN	54
DISCUSSION	54
EXPERIMENTAL TECHNIQUES	56
RESULTS AND INTERPRETATION	59
INTERNAL FRICTION STUDIES	66
DISCUSSION	66
EXPERIMENTAL TECHNIQUES	67
RESULTS AND INTERPRETATION	70

HIGH TEMPERATURE STUDIES	78
DISCUSSION	78
EXPERIMENTAL TECHNIQUES	81
SUMMARY & CONCLUSIONS	85
APPENDIX A	89
PRE-YIELD STRAIN AND STRESS INDUCED DIFFUSION IN BCC METALS	89
APPENDIX B	99
STRAIN OR STRESS INDUCED CHANGE IN THE ACTIVATION ENERGY OF INTERSTITIAL DIFFUSION	99
APPENDIX C	109
EFFECT OF THE STRESS FIELD OF DISLOCATIONS ON INTERSTITIAL DIFFUSION	109
APPENDIX D	114
MAGNITUDE OF ANELASTIC STRAIN NORMAL TO THE APPLIED STRESS	114
APPENDIX E	
ACTIVATION ENERGIES DEFINING THE YIELD DELAY TIME AND THE MICROSTRAIN RATE	117
REFERENCES	119

LIST OF ILLUSTRATIONS

<u>FIGURE</u>		<u>PAGE</u>
1	Electron Beam Melted Tantalum	24
2	Electron Beam Melted Columbium	25
3	Test Chamber of Tensile Unit Modified for Vacuum Operation	26
4	Facility for High Speed, High Temperature Tensile Experiments	27
5	Typical Yield Delay Experiment	32
6	Typical Yield Delay Recovery Experiment	33
7	Stress Rate Dependence in Recrystallized Tantalum (Rate Constant to Yield)	38
8	Stress Rate Dependence of Recrystallized Columbium (Rate Constant to yield)	39
9	Yield Delay in Recrystallized Tantalum	40
10	Yield Delay in Recrystallized Columbium	41
11	Linear Microstrain Rate in Recrystallized Tantalum	42
12	Linear Microstrain Rate in Recrystallized Columbium	43
13	X-Ray Diffraction Unit	58
14	Internal Friction in Recrystallized Tantalum (Nominal Resonance Frequency 67 cps)	71
15	Internal Friction in Recrystallized Tantalum (Nominal Resonance Frequency 36 cps)	72
16	Internal Friction in Recrystallized Columbium (Nominal Resonance Frequency 250 cps)	73
17	Internal Friction in Recrystallized Columbium (Nominal Resonance Frequency 66 cps)	74
18	Tantalum & Columbium - Recrystallized after 75% cold Reduction	84

INTRODUCTION

The specific purpose of this investigation was to establish the presence of delayed yield, pre-yield microcreep and related strain rate effects in tantalum and columbium and to determine the major mechanisms controlling these effects. From previous experiments on molybdenum, another body centered cubic metal, it was established that interstitial impurities, by a mechanism analogous to the Snoek effect, contribute significantly to the pre-yield microcreep, and apparently play a controlling function in the yield delay and strain rate sensitivity of the material. A major portion of the present investigation was devoted to detect similar phenomena in tantalum and columbium. The contributions made by interstitials to the anelastic behavior of bcc metals may be summarized in the following manner:

In a typical yield delay experiment the interstitials contribute to the anelastic pre-yield deformation (microcreep), by diffusion controlled reorientation of interstitials into preferred lattice sites. Consequently, microcreep can be considered a result rather than cause of yield delay.

The diffusion phenomenon itself should also have a controlling effect on the yield delay time by reducing potential and actual barriers to the propagation of dislocations in preferred slip planes and by reducing Cottrell atmospheres about dislocations.

Manuscript released by the authors Nov 1962 for publication as an ASD Technical Documentary Report.

In the case of strain rate experiments a similar model can be hypothesized. During the load application, diffusion of interstitials into preferred positions takes place simultaneously with the elastic deformation. Depending on the relative rates of the diffusion and of the elastic lattice strain, the reduction of barriers and Cottrell atmospheres prior to yield will vary, resulting in a variation of the upper yield point with strain rate.

This model is basically not in conflict with the dislocation model of anelasticity but complements the latter. The dislocation models of yield delay have, to date, given no consideration to redistribution of interstitials; but, it has long been established, first by Snoek, that this is a real phenomenon. To establish whether the proposed impurity model has validity the following experimental evidence was to be established. First, the activation energy of microcreep must have functional dependence on the activation energy of diffusion of the interstitials present. Secondly, non-elastic lattice deformation due to reorientation of interstitials, and not only slip deformation due to dislocation motion, must be present during the pre-yield deformation process. Thirdly, the upper yield point, either in yield delay or strain rate experiments, must show a dependency on the activation energy of interstitials.

It is obvious that the diffusion rates of most common interstitials in the lattice either at very low or very high temperatures, are such that

preferential reorientation is either too slow or too fast to produce any observable anelastic effects. This is easily understood if we define anelasticity as the condition at which strain is lagging the applied load in time, or, at which the strain is out of phase with the applied stress. Therefore, this portion of the investigation was confined to the low and medium temperature range (-100°F to $+400^{\circ}\text{F}$) for both tantalum and columbium.

The second phase of this investigation is aimed at high temperature anelastic behavior of tantalum and columbium. The extent of this phase is such that it must be considered an initial effort only, for the purpose of establishing experimental methods and exploratory data.

At high temperatures the causes for anelasticity in bcc metals have not as yet been precisely defined. Even the characteristics of anelasticity at high temperatures have only been very sketchily observed. Primary indications that anelasticity does in fact exist comes only from a number of experiments indicating the re-appearance of upper yield points at very high temperatures and the presence of strain rate sensitivity. From the previous experiments it appeared justified to anticipate a direct relation between these two phenomena and anelasticity. As stated earlier, interstitial impurities, at least in small concentrations, cannot be expected to produce anelastic behavior at high temperatures except, perhaps, in cold worked metals. It was, therefore, important to first hypothesize

and experimentally verify which basic material properties or constituents can contribute to anelastic behavior. Based on estimated activation energies and other evidence a number of contributors can be anticipated: substitutional impurities, grain boundaries by means of grain boundary viscosity, pairs or larger aggregates of interstitials in saturated metals, and possibly dislocations moving with their impurity atmospheres or slowed down by specific barriers. High temperature internal friction studies, yield delay and strain rate experiments, as well as careful control of the material properties, are considered the basic requirements to approach the problem. To prevent the various possible contributors to anelasticity from producing undue complexity of the problem it was decided to use grain size variation as the first variable parameter in this investigation.

THEORETICAL BACKGROUND

DISLOCATION MODEL

Most of the recent theories on the anelastic, pre-yield behavior of bcc metals, e.g., iron⁽¹⁾ and molybdenum⁽²⁾, are based on a pure dislocation model. Basically the assumption is made that, during yield delay, a number of dislocations propagate in slip planes with suitable orientation, relative to the applied stress, and thus cause an observable microcreep rate. Depending on the applied stress, the extent of propagation of the dislocations is limited by barriers in the material, such as grain boundaries. Dislocations pile up at these boundaries until their combined stress is sufficient to overcome these barriers, thus causing macroscopic yield. The time required to generate a sufficient number of dislocations for the initiation of macroscopic yield is identified as the yield delay time. This concept was originated by Fisher who derived appropriate relations⁽³⁾ introducing the activation energy for the nucleation of the dislocation loops from their Cottrell atmospheres during the pre-yield deformation. These relations were later modified by Vreeland and Wood⁽⁴⁾ to include the effects of backstress of the activated dislocation loops.

In their simplest form, based on the original work by Fisher, these relations may be expressed as

$$\begin{aligned} t_y &= A e^{\frac{\gamma_0^2 f(\gamma/\gamma_0)}{b \sigma_1 R T}} \\ \dot{\epsilon}_0 &= B e^{-\frac{2 \gamma_0^2 f(\gamma/\gamma_0)}{b \sigma R T}} \end{aligned} \quad (1)$$

where τ_y = time to yield
 $\dot{\epsilon}_0$ = initial microstrain rate
 A, B = factors relatively insensitive to temperature and stress
 γ_0 = energy per unit length of dislocation when free from solute atoms
 γ = energy per unit length of dislocation in the presence of solute atoms
 b = Burgers vector
 σ_1, σ = the applied shear and tensile stress, respectively

$$f(\gamma/\gamma_0) = \cos^{-1}(\gamma/\gamma_0) - \gamma/\gamma_0 (1 - \gamma^2/\gamma_0^2)^{\frac{1}{2}}$$

It may be specifically noted that these expressions imply that the logarithm of the delay time as well as of the microstrain rate are inversely proportional to the applied stress. When experimental data were fitted to these theoretical expressions by Vreeland and Wood, it was found that the empirical values of $f(\gamma/\gamma_0)$ led to unusually small values of

$1 - \gamma/\gamma_0$. When compared with the energy ratios calculated by Cottrell a discrepancy of a factor of 50 was determined in the case of iron. This large factor may be reduced somewhat by introducing the suggestion by Cottrell ⁽⁵⁾ that the dislocation segments involved in the yielding process may be significantly smaller than the length of Frank Read source. For example, the existence of active dislocation elements of a length of approximately 10 b, is suggested by the work of Mura and Brittain ⁽⁶⁾. However, with these dimensions the line energy of the active dislocation is changed by a factor of about two only and does not nearly account for the observed discrepancy.

Several investigators have since proposed that the preyield deformation process is controlled by an activation energy which is a linear function of the applied stress rather than an inverse function.

For example, Peiffer⁽⁷⁾ in a recent analysis indicates that the yield delay time should be described by a relation similar to that derived by the authors during earlier work on molybdenum⁽⁸⁾.

According to Peiffer

$$\frac{1}{T} = \frac{\nu_0}{N} e^{\frac{-E_0 - \nu\sigma}{RT}} \quad (2)$$

where ν_0 = Debye frequency

N = number of dislocation segments that have moved before macroscopic yielding occurs

E_0 = activation energy

ν = activation volume of dislocation.

Peiffer used the same experimental data which yielded an apparent verification of Relations (1) to show the applicability of Equation (2).

Some insight into the question of whether one would expect Cottrell's dislocation model to apply has been thought to be obtainable from measurements of the variation in lower yield stress with average grain diameter for different temperatures. The usual Petch type equation $\sigma_y = \sigma_i + k_y d^{-1/2}$ would be expected to apply. In this equation $k_y = \sigma_0 l^{1/2}$ is a measure of the stress required ahead of an equilibrium dislocation pile-up to

unlock a Frank-Read source from its Cottrell atmosphere.

We refer to an excellent review for the temperature dependence of each of the component expressions in the Petch equation ⁽⁹⁾. It has been concluded that the sharp increase in the yield point with decrease in temperature is not connected with the fastening of dislocations by the Cottrell "clouds".

In particular, the k_y factors in tantalum ⁽¹⁰⁾ and columbium ⁽¹¹⁾ appear to be by a factor of six to ten smaller than in iron or molybdenum. This implies that the Cottrell locking in the two metals (Ta, Cb) is very weak indeed.

Strong temperature dependence of the upper yield stress is not in agreement with such a conclusion. It was therefore felt that, at least at the upper yield point, the Cottrell mechanism is still a controlling factor in the bcc metals under investigation. Since yield following yield delay occurs somewhere between the upper and lower yield point, by the usual definition, it must be assumed that Cottrell or other interstitial - dislocation interactions must be given consideration. Also, observations of the Bordoni peaks by various investigators point toward efficient interstitial locking ⁽¹²⁾.

The relative insensitivity of k_y signifies the existence of some athermal mechanisms in the yield process in addition to or in place of the thermally activated unpinning of dislocations. This was pointed out by Conrad and Schoeck ⁽¹³⁾. The k_y factor may, e.g., describe the athermal generation

of dislocations in or near grain boundaries from sources other than the Frank-Read type source.

INTERSTITIAL DIFFUSION MODEL

A critical, theoretical evaluation of all available data was initiated to establish whether the pure dislocation model of pre-yield anelasticity, and its inherent uncertainties, could either be reconciled with or replaced by a model, as formerly suggested^(8, 14, 15), which takes into account the contribution of interstitial diffusion.

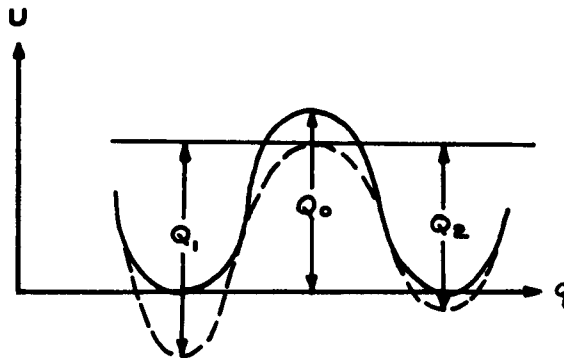
Previous work on molybdenum⁽⁸⁾ resulted in a semiempirical description of the observed microcreep and strain rate data which had the form

$$\epsilon_t = \frac{\sigma(t)}{E_u} + K r_i n_i \int_0^t e^{-\frac{Q - \ell \sigma(t)}{RT}} e^{-\lambda n t} dt \quad (3)$$

The first term on the right side of the equation corresponds to the purely elastic strain and the integral to the time dependent anelastic strain caused by reorientation of interstitials for an arbitrary stress history. A complete derivation of Equation (3) is given in Appendix A.

Though Equation (3) provides a suitable description of experimental data both for microcreep and strain rate sensitivity, it did not yield an entirely satisfactory theoretical interpretation of these data. The activation energies, Q , for iron,⁽¹⁶⁾ molybdenum⁽¹⁷⁾, and columbium⁽¹⁸⁾ appear to indicate beyond any doubt that interstitial diffusion represented a controlling mechanism. However, the value of, ℓ , is in all cases an order of magnitude or more greater than could be calculated, by basic thermodynamic theory, from the change of energy with strain $\partial u / \partial \epsilon$,

of an interstitial in its preferred, non-preferred, or saddle point position.



Appendix B contains a discussion of the effect of stress on diffusion rates together with calculations of ℓ as based on experimental information on the martensitic transformation in bcc metals.

Numerous variations of Equation (3) were investigated based on other empirical descriptions of both the yield delay and strain rate phenomena. For example, it can be shown that, over the normal range of stresses in yield delay experiments, the data obtained in this investigation can also be represented either as linear or inversely proportional functions of stress e.g., $\ell \dot{\epsilon} \propto \sigma$ or $\ell \dot{\epsilon} \propto \frac{1}{\sigma}$. Both produce apparently straight line relations for any given temperature. It was feasible to satisfactorily fit the experimental data obtained in this investigation to these and other relations, at least over a major portion of the stress ranges used. However, none of the forms suggested to date provide a non-empirical interpretation of the experimental data if a pure interstitial model is used.

PROPOSED MODEL, DISLOCATION - INTERSTITIAL INTERACTION

A re-evaluation of the yield delay model led to a satisfactory solution.

It was concluded that the pre-yield deformation mechanisms must indeed be described by the combination of a dislocation and interstitial diffusion model.

The stress levels causing yield delay are always sufficiently high to activate a number of dislocation segments. The probability that dislocation segments are propagated from their source is governed by the jump frequency which is an exponential function of the activation energy Q_D . The latter is determined by immediate barriers such as Cottrell atmospheres and the Peierls barrier of the material. The jump frequency is enhanced, or the activation energy lowered, by the application of a stress. The fact that dislocation motion is a jump process has been demonstrated experimentally⁽¹⁹⁾.

During microcreep, the length of the dislocation segments free to move under the applied stress is determined by the density of the interstitials locking the dislocation. In Appendix C it is shown that interstitials below a positive dislocation, provide maximum locking, and that, on application of a stress, interstitial positions in the slip plane correspond to preferred positions relative to the positions below the dislocation.

Consequently, if the applied stress is less than the upper yield point, the propagation of the line segments is possible only if the interstitials in the locking position diffuse into preferred positions under the influence of the applied stress. Therefore, the motion of each dislocation segment is controlled by the probability that an interstitial is not present in the locking position.

This may be expressed as

$$\frac{dN_D}{dt} = -\lambda_D N_D (1 - e^{-t\lambda_I}) \quad (4)$$

Where

N_D = number of dislocation segments blocked by interstitials from propagating a primary distance, d .

λ_D = effective decay constant (or jump frequency) of dislocation segment not locked by interstitial

λ_I = effective decay constant of interstitial into neighboring, vacant site.

The decay constant λ_I , must be considered in the light of the interstitial - dislocation interaction, and of the effects of an applied stress.

Now, using the same notations as used elsewhere for interstitial diffusion

$$(\frac{1}{24})\lambda_I = D_I/d^2 = D_0 e^{-\frac{Q_I}{RT}}/d^2$$

it has already been shown in the discussion on the pure interstitial diffusion model and in Appendix A that the activation energy Q_I has a stress dependency $Q_I = Q_0 - \ell \sigma$, where ℓ only depends on the lattice strain. It has also been shown that the drift velocity of impurity atoms is affected by the stress field of the interstitials themselves.

This can be expressed in terms of $v_I = (D_I/RT)F$ (5)

The force term F , due to the static stress field of a dislocation is normally defined as A/r^2 , where r is the distance between the interstitial and the dislocation and A is a constant which depends on: the misfit of the interstitial, ϵ ; the shear modulus, μ ; the burger vector, b ; and the radius of the host atoms, r_0 . An early definition of A , by Cottrell, is of the form $A = 4\mu b \epsilon r_0^3$. Mura et al, ⁽²⁰⁾ have shown that the force factor F is in addition an apparently linear function of the applied stress. They postulated that the applied stress increases the length of the unpinned portions of the dislocation by bulging. This in turn affects the line tension of the dislocation and consequently its interaction with impurities. Thus $U_I = \sigma(D_I/RT)F'$

It was then theorized that during the pre-yield deformation process the dislocation will also affect the energy of the interstitials in various interstitial positions near a dislocation and, as a result, produce preferred positions into which the interstitials will diffuse and permit the dislocation to propagate.

The mathematical formulation of this theory is presented in Appendix C. It is shown that a difference in the activation energy of diffusion exists which is directly proportional to the temperature and the applied stress. As shown in Equation (C5).

$$\Delta V = - \frac{b a^3 \sigma_3 RT}{4 \pi C_I A} \quad (6)$$

This leads to a diffusion coefficient of the form

$$D_{ID} = \lambda_I \frac{d^2}{24} = f \sigma D_0 \exp \left(- \left(\frac{Q_0 - \ell \sigma}{RT} - \beta \sigma \right) \right) \quad (7)$$

Equation (7) has considerable consequences and removes the empiricism introduced by Equation (3). In the latter equation the coefficient ℓ was shown theoretically to be entirely too small (Appendix B) to account for experimentally observed stress effects. Also all experimental data including those presented in this report show that the stress effect on the activation energy is very temperature insensitive over the observed range.

It must also be cautioned here that λ_D is not independent of the interstitials after unlocking has taken place. Interstitials in the slip plane, e.g., though not participating in the locking process do exert a force on the dislocation and, thus, influence its motion. Such a consideration will require a modification of the treatment by Seeger et al⁽²¹⁾ who have expressed the rate of formation of unlocked dislocation bulges by

$$v = A \exp \left(-H/KT \right) \quad (8)$$

Here, A is just the frequency of oscillation of a dislocation in the Peierl's potential well and H the corresponding activation energy. A should be modified to include the force effect due to interstitials located in the slip plane in the neighborhood of the dislocation.

Starting with Equation (4), both the time to yield and the microstrain rate prior to yield can now be defined.

Equation (4) can be rearranged to read

$$\frac{dN_D}{N_D} = -\lambda_D (1 - e^{-t\lambda_I}) dt \quad (9)$$

which can be immediately integrated. Utilizing the approach of the pure dislocation model which assumes that a critical number of dislocations must be propagated before macroscopic yield occurs, we can define the limits of integration by

$$N_D = N_{D0} \quad t = 0$$

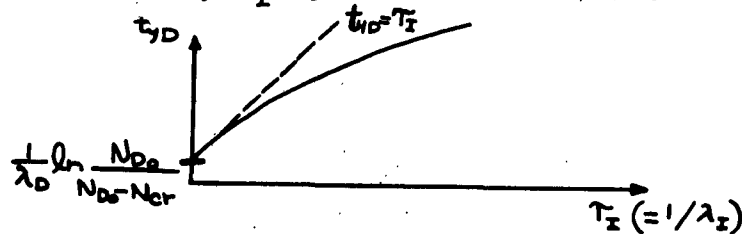
$$N_D = N_{D0} - N_{cr} \quad t = t_y \text{ (the yield delay time)}$$

Integration over these limits yields

$$\ln \frac{N_{D0}}{N_{D0} - N_{cr}} = \lambda_D \left[t_y - \frac{1}{\lambda_I} (1 - e^{-\lambda_I t_y}) \right]$$

$$\text{or} \quad t_y = \frac{1}{\lambda_I} (1 - e^{-\lambda_I t_y}) + \frac{1}{\lambda_D} \ln \frac{N_{D0}}{N_{D0} - N_{cr}} \quad (10)$$

The relative dependence of the yield delay time on the interstitial diffusion mechanism is quite obvious from Equation (10). The following graph indicates the relationship, (noting that λ_I is inversely proportional to the time constant, τ_I , of the interstitial jump mechanism).



With this result the description of the pre-yield microstrain and strain-rate can now also be reconciled with all experimental data. It is still maintained that microstrain occurs due to the redistribution of interstitial atoms into preferred positions. This redistribution is the result both of the strained lattice and the dislocations attempting to propagate under the applied stress during preyield shear deformation.

The microstrain is a function of the misfit or size of the interstitial atoms, the average lattice orientation of the metal under investigation, and, of course, the density of the interstitials. The microstrain rate can be defined as before (Appendix A) by

$$\dot{\epsilon} = C r_I \dot{n}_I = C r_I \lambda_I n_I e^{-\lambda_I t} \quad (11)$$

with the modifications for the interstitial-dislocation interactions this leads to

$$\dot{\epsilon} = C n_I r_I \sigma F' D_0 e^{-\frac{Q_0 - \lambda \sigma}{RT}} e^{-\lambda_I t} \quad (12)$$

which, as observed, is constant during the initial portion of a yield delay experiment, i.e., when $\lambda_I t \ll 1$. The constant, C , is primarily a function of the distribution of the lattice orientations.

(22)
It may be noted that Professor Dorn showed experimentally that the stress effect on the activation energy of creep (macroscopic) behaves in a similar manner, i.e., is apparently independent of temperature.

Equation (12) shows also that if the time τ becomes large relative to λ_{τ} the strain rate approaches zero.

It is noteworthy that during numerous experiments the strain rate indeed approached zero prior to yield. If the observed microstrain was primarily due to the propagating dislocations it is difficult to conceive that yield should have occurred after the propagation or generation of the dislocations had ceased. On the other hand it is very conceivable that the primary locking interstitials in non-preferred positions will become exhausted or reach an energy equilibrium with those in the preferred position. While this will terminate the process of anelastic straining, the dislocations will continue to propagate under the applied stress until yield occurs. The speed of these dislocations will then be controlled by other imperfections including the effects of interstitials not in locking position as discussed previously.

Of interest for the evaluation of experimental data and the definition of the interstitials are the activation energies of both the yield delay time and the microstrain rate. The format of Equations (10) and (12) indicates that a simple expression for the activation energy does not exist, except under certain conditions when first order approximations can be introduced. For the general case we may consider effective activation energies defined by

$$\begin{aligned} t_y &= A e^{Q'_{eff}/RT} \\ \dot{\epsilon} &= B e^{-Q''_{eff}/RT} \end{aligned} \quad (13)$$

In Appendix E the effective activation energies are calculated for both processes. The results are

$$Q'_{eff} = \frac{Q_I - Q_D}{\lambda_I t_y} + \frac{Q_D - Q_I e^{-\lambda_I t_y}}{1 - e^{-\lambda_I t_y}} \quad (14)$$

$$Q''_{eff} = Q_I (1 - \lambda_I t) \quad (15)$$

It can be seen that both effective activation energies are temperature sensitive even if only one type of interstitial participates in the process. This temperature sensitivity increases considerably when more than one type of interstitial, each with its own activation energy of diffusion, participates. The effective activation energies for either process are then given by

$$Q_{eff} = \frac{\sum_i \omega_i \lambda_i Q_i (1 - \lambda_i t) e^{-\lambda_i t}}{\sum_i \omega_i \lambda_i e^{-\lambda_i t}} \quad (16)$$

where the Q_i 's and ω_i 's are the effective activation energy and weight factor, respectively, of the i th diffusion process. The weight factors are primarily determined by the relative initial density of all interstitials participating in the dislocation locking process.

The generalized expression of Equation (16) and Equations (14) and (15) indicate that, 1) as the temperature is varied different types of interstitials will make the primary contribution to the preyield anelastic deformation process; 2) at any given temperature, the length of the preyield deformation process, i.e., the time to yield determines how many types of interstitials may have significant effects.

It is obvious if the activation energies of two or more types of interstitials are of nearly equal magnitude, they will all contribute simultaneously to the anelastic behavior independent of time and temperature.

The temperature dependence of the various activation energies is analogous to the experimental findings of Professor Dorn ^(22) who has shown that the activation energies for creep (macroscopic) are very temperature sensitive until a temperature is reached such that apparently the self diffusion provides the only controlling mechanism. After that the activation energy is constant with respect to temperature over the range of observation.

To summarize, the following conclusions have been reached based on theoretical considerations and influenced by all experimental results to date on the preyield anelastic behavior of bcc metals containing traces of interstitials:

The time to yield during yield delay experiments is determined by the capability of locked dislocations to move out of their interstitial atmosphere. Consequently, the jump frequency of interstitials out of locking

positions into preferred positions has a controlling effect on the yield delay time. This is compatible with previous, pure, dislocation models which define the time to yield as the time required to propagate a critical number of dislocations.

Preyield microstrain is a direct result of the interstitial reorientation. A Snoek model does not suffice to describe this reorientation mechanism. Dislocations, under an applied stress, have a much greater effect on the activation energy of diffusion than the elastically strained lattice. The resulting effect on the jump frequency of the interstitials is very insensitive to temperature. It has also been shown that the activation energies are linear functions of the applied stress.

The effective activation energies based either on the yield delay time or the microstrain rate, are both temperature and time dependent. These dependencies become very significant if more than one type of interstitial is present in the metal under investigation.

TENSILE EXPERIMENTS

DISCUSSION

The first objective of the tensile experiments was to establish the presence and magnitude of yield delay and pre-yield micro creep in tantalum and columbium in the medium temperature range. The second and more important objective was to obtain as much insight as possible into the basic mechanisms and properties controlling the anelastic phenomena in these two bcc metals.

When designing the experiments, the basic assumption was made that the pre-yield anelastic deformation follows an Arrhenius type behavior, i.e., all time dependent mechanisms are functions of a characteristic activation energy. This is, of course, the same assumption which results from the theoretical background discussion. Therefore, the determination of the activation energies, as well as their dependence on temperature and on the applied tensile stress, became a primary goal of this work.

The activation energies of interest are those of the microcreep with stress applied to the specimen, of the time to yield again with the stress applied, and of the recovery of any nonelastic strain on removal of the load.

As in any experimental effort, the influence of uncontrolled parameters had to be prevented. In this case this required identity of each set of specimens with respect to mechanical history, pre-experimental heat

treatments, and constituents. It also required that any internal stress introduced during specimen preparation be removed. Because an extensive parametric study on single crystal tantalum and columbium was economically unfeasible, it was desirable to use specimens of rather small grain sizes with random orientation.

It was possible to meet most of the objectives of the tensile experiments with the exception of obtaining quantitative results from the yield delay recovery experiments. The relatively slow speed of the thermal diffusion process prevented the establishment of a rigorous time scale for the recovery in this set of experiments.

EXPERIMENTAL TECHNIQUES

Specimens

The specimens for all tensile experiments were of identical geometry; 0.25 inches in diameter by 10 inches long. The center six inches were reduced to a diameter of 0.245 inches. The round configuration was chosen to minimize the surface to volume ratio. The length of the specimens was determined from thermal considerations and represents the minimum length at which the temperature gradient over a two inch gage length is negligible for all temperature conditions imposed. The reduction of the center portion of the specimens is only necessary for experiments below room temperature

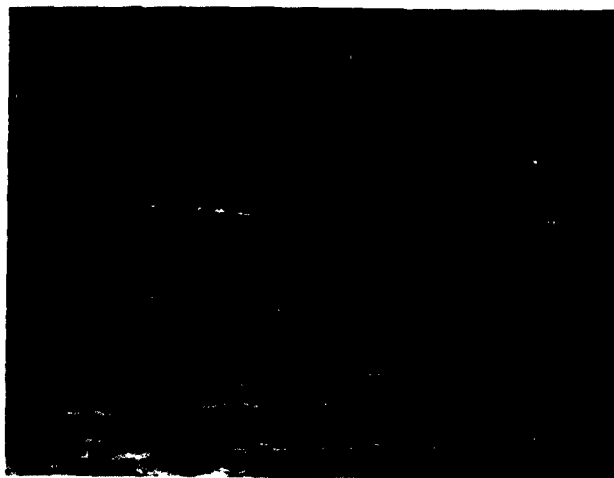
and prevents yield and necking outside the gage length. Above room temperature the gage length is at a temperature sufficiently higher than that of the other portions of the specimen to guarantee initiation of yielding near the center without reduction of geometry. However, all specimens were machined to the same dimensions to obtain identical coldwork.

The chemistry of both the tantalum and columbium was carefully checked, in the vendors laboratory, prior to delivery and prior to the experiments, i.e., after the completion of pre-experimental specimen preparation. The material was electron beam melted and delivered in stress relieved form. The following tables give the results of the vendors analysis (Wah Chang Corporation, Albany, Oregon). Only the more important interstitial components were re-analyzed prior to the experimental program.

	<u>Tantalum</u> ppm (by weight)		<u>Columbium</u> ppm (by weight)	
Al	20		20	
B	1		1	
Cb	500		Ta 470-490	
Co	20		ND	
Cr	20		20	
Cu	40		40	
Fe	100		100	
Hf	ND		ND	
Mg	20		20	
Mn	20		20	
Mo	20		20	
Ni	20		20	
Pb	20		20	
Si	100		100	
Sn	20		20	
Ti	150		150	
V	20		20	
W	300		65-72	
Zn	20		20	
Zr	500		500	
	<u>Original</u>	<u>Final</u>	<u>Original</u>	<u>Final</u>
C	30(50)	80	30(90)	30
N	55(100)	35	72-99(85)	26
O	50(85)	105	110-180(150)	50
H	ND(4.3)	3.2	2.2-2.3(6.0)	3.0

Data in parentheses represent reanalysis of as delivered specimen material prior to experiments.

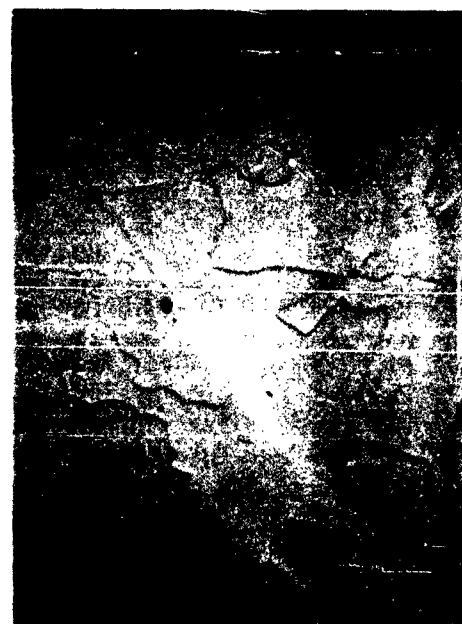
ELECTRON BEAM MELTED TANTALUM



a. AS RECEIVED (x 75)



b. LONGITUDINAL

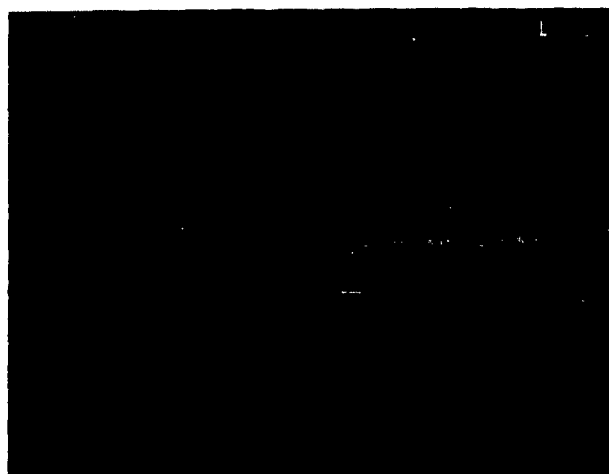


c. TRANSVE.

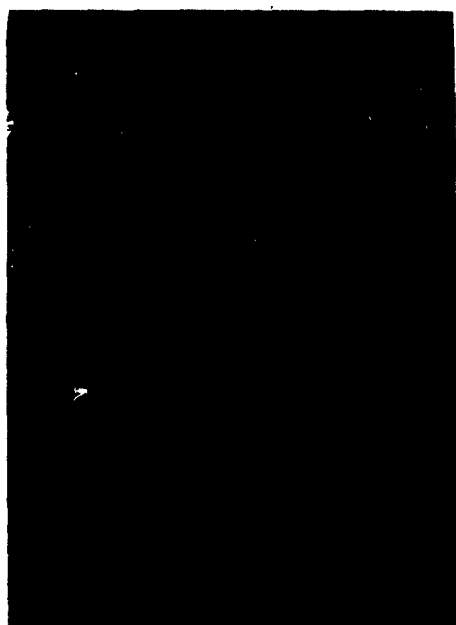
RECRYSTALLIZED - 1 HR AT 1200°C (X 150)

Figure 1

ELECTRON BEAM MELTED COLUMBIUM



a. AS RECEIVED (x 75)



b. LONGITUDINAL



c. TRANSVERSE

RECRYSTALLIZED - 1 HR AT 1200°C (X 150)

Figure 2

TEST CHAMBER OF TENSILE UNIT MODIFIED
FOR VACUUM OPERATION

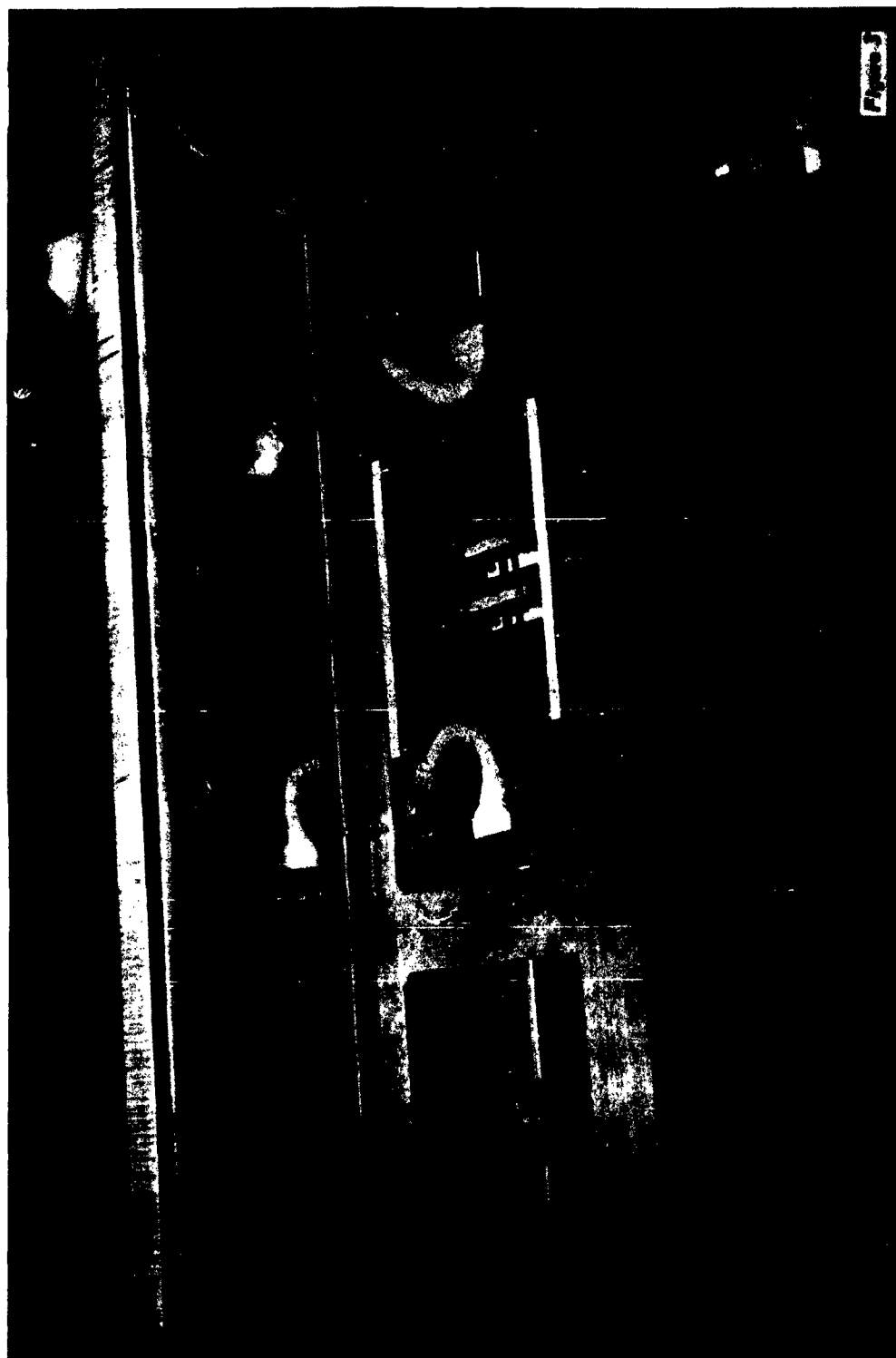
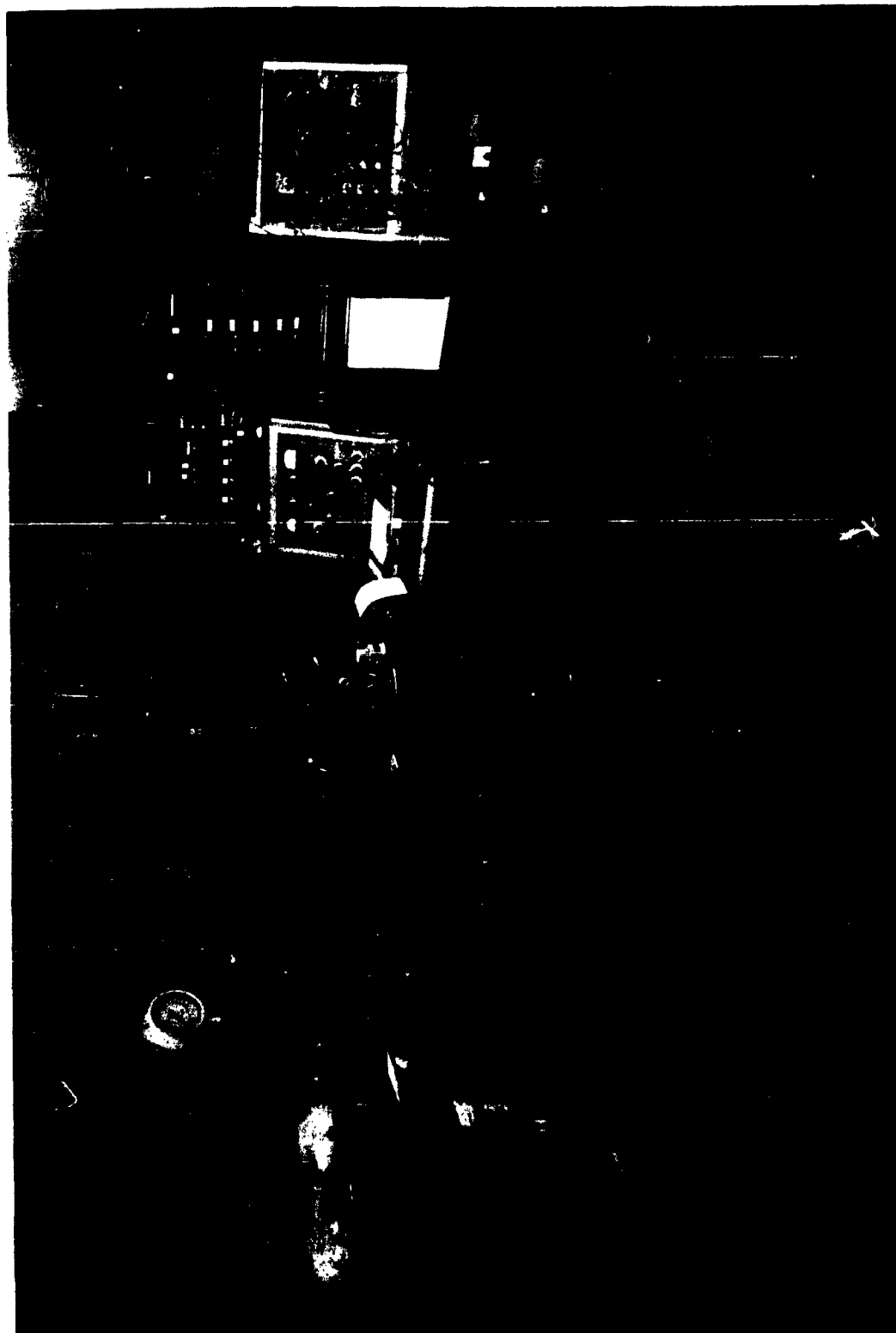


Figure 4 FACILITY FOR HIGH SPEED, HIGH TEMPERATURE
TENSILE EXPERIMENTS



As stated above, both tantalum and columbium were received in stress relieved form for best machineability. On machining to the final geometry the specimens were recrystallized at 1200^o C for one hour in a dry air environment at less than .3 micron Hg pressure. The material was slow cooled to prevent recurrence of internal stresses due to thermal gradients. Figures 1a through 2c illustrate the initial and final structure of both materials. Comparing the photomicrographs of the final longitudinal and transverse structures (specimen axis being the reference) it can be seen that the original directionality in grain-structure has disappeared.

Equipment

All tensile experiments were performed on a high temperature, rapid load tensile unit designed and developed at General Dynamics/Pomona. The basic components of this unit are a load dynamometer, templin type grips, an extensometer, a hydraulic cylinder, a servo valve, a servo feed back system, and a powerstat with step down transformer for the temperature control. All tensile components are mounted in a loading frame designed for high impulse loading. This frame can be sealed for operation in an inert atmosphere, in liquid coolants, or in a vacuum. Figures 3 and 4 show the physical arrangement of the equipment.

Either the load rate or the strain rate can be controlled. Within the limits of the performance characteristics, load, strain and temperature histories can be programmed and automatically applied to the specimen.

The load dynamometer serves to measure the instantaneous load on the specimen as well as to provide a servo feedback signal during programmed load cycles. At present, dynamometers for two load ranges are available, 0-3000 lb and 0-15000 lb. The accuracy for each unit is 0.5%.

The templin type grips were considered very advantageous for this investigation. Due to their ability to distribute the applied loads uniformly over the gripping area of the specimen, a simple rod (or reed) configuration provides a satisfactory specimen geometry. There is no need for complex shapes such as threaded, pinhole or shouldered specimens. This eliminates the need for excessive cold work and is also an important factor when working with expensive materials, such as pure tantalum and columbium. The presently available grips can accommodate round specimens of 0.25 inch diameter or flat specimens from 0.020 to 0.125 inches thick.

The extensometer used in this work was specifically designed for this task. It consists of a light weight structure suspended on knife edges from the specimen with sufficient pressure (spring loaded) to prevent slippage problems during rapid load application. Strains are measured with an accuracy of 0.5% over a gage length of 2 inches. The extensometer also provides the feedback signal to the servo system for automatic strain history control.

The hydraulic cylinder, the servo feedback control system and the servo valve provide the load inputs which range from effectively step loads to

several pounds per hour (or slower by manual step control). The corresponding strain rate inputs range from 0.00001 to greater than 0.01 inch per inch per second.

The specimens are heated either by immersion in a circulating fluid at low temperatures or by resistance heating at high temperatures. The specimen itself represents the heating element. Radiation shielding and grip insulation minimizes temperature gradients in the specimen. Specimen temperatures and heating rates are controlled by the powerstat and stepdown transformer. The temperature range of the unit is presently -107°F to 6000°F . Heating rates up to 1000°F per second can be obtained during resistance heating.

Temperatures can be maintained within better than 1°F over extended periods of time. The accuracy of the temperature reading is that of thermocouples for the appropriate temperature range. The thermocouples are spotwelded on the specimen and calibrated prior to the experiments.

The data are presented on three types of recorders; Sanborn, direct-read-out C.E.C., and Moseley. The various recordings serve to countercheck measuring techniques if anomalous specimen response is observed.

The Sanborn and C.E.C. recorder display load, strain, and, when desirable, temperature as a function of time. The C.E.C. unit, having the fastest response time serves as the primary recorder of the experimental data

which are to be evaluated. The Mosely recorder provides an accurate backup for stress and strain calibration, and is also very useful in relatively slow experiments for the determination of the yield point (elastic limit).

Experimental Procedure

Three types of experiments were performed: constant load rate, yield delay, and yield delay recovery.

The constant load rate experiments established three characteristics, yield stress as a function of temperature, yield stress as a function of constant stress rate, and, consequently, time to yield under various rate conditions. This set of experiments was primarily of exploratory value. It was established earlier with molybdenum⁽⁸⁾ that if a stress is applied as rapidly as possible and maintained constant, the yield delay time is very nearly the same as the time to yield in a load rate experiment if the resulting yield stress is of the same magnitude.

With a minimum of data points it is thus possible to establish for various temperatures the stress levels at which yield delay times of reasonable length can be expected.

In this fashion it was determined that, contrary to the original intention of operating above room temperature only, yield delay experiments had to be carried out between -20°F and $+400^{\circ}\text{F}$ in tantalum and -100°F and $+150^{\circ}\text{F}$ in columbium to obtain meaningful, observable data.

Figure 5 TYPICAL YIELD DELAY EXPERIMENT

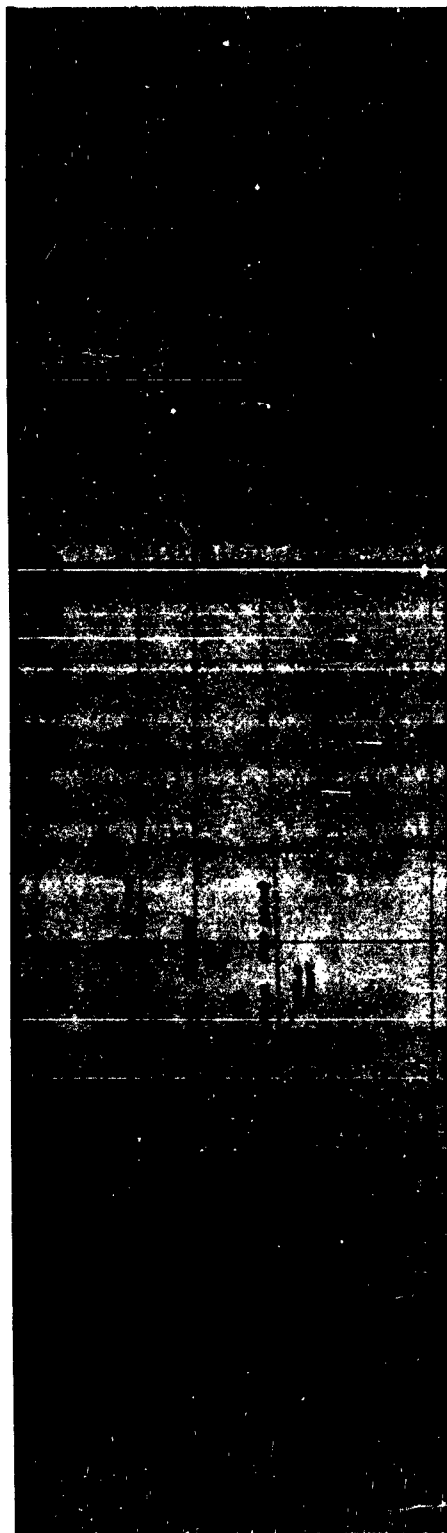
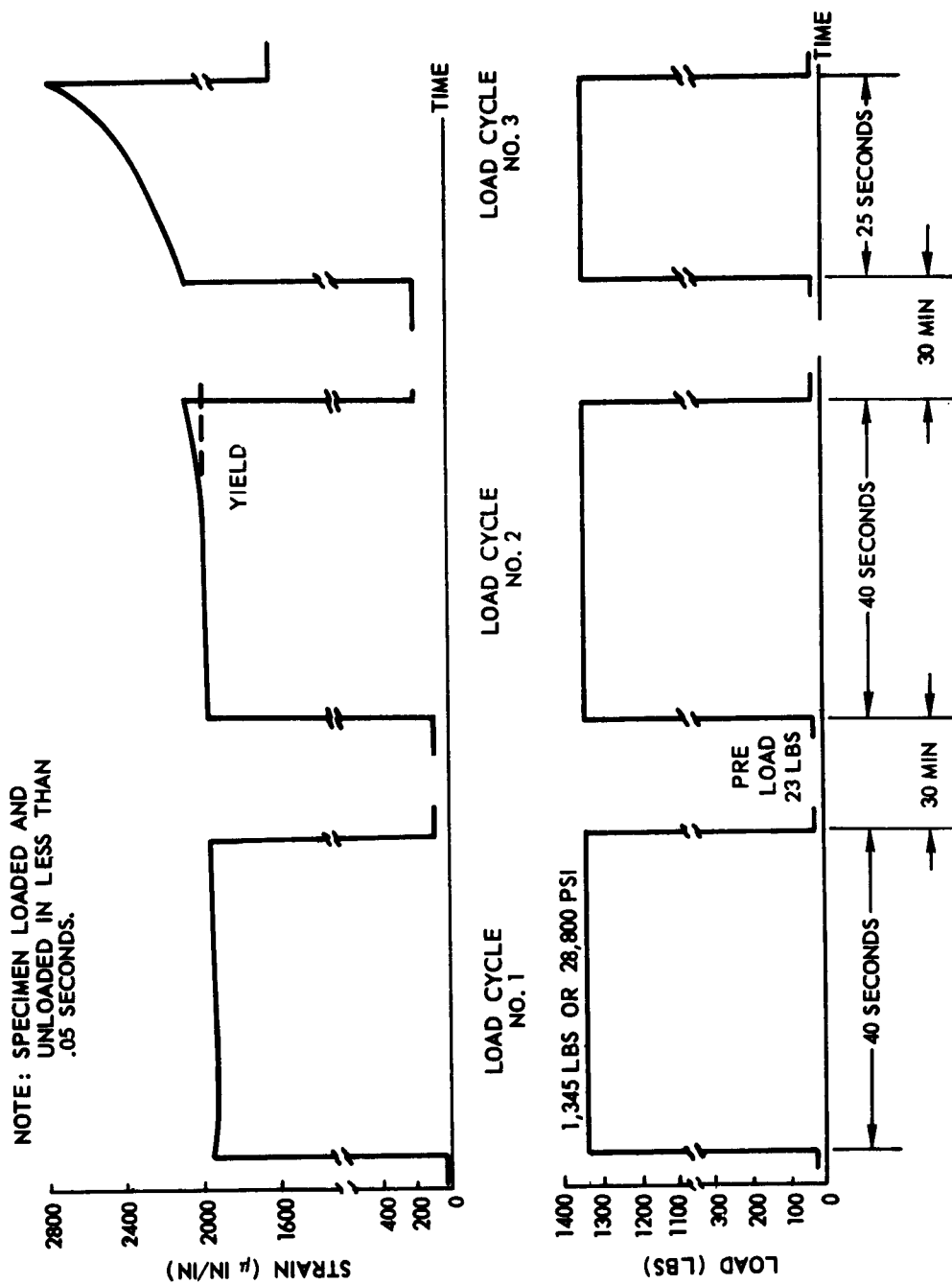


Figure 6 TYPICAL YIELD DELAY RECOVERY EXPERIMENT
COLUMBIUM C-79 TEST TEMPERATURE -20°F
LOAD AND STRAIN VS TIME



Figures 7 and 8 show the useful data for tantalum and columbium respectively. Equivalent stress rates varying from 1 PSI per second to 2.5×10^6 PSI per second were applied.

A typical yield delay experiment is shown in Figure 5. The stress is applied as rapidly as possible and then maintained constant until yield occurs. The maximum applicable stress rate was a function, not of the energy reservoir or time response of the hydraulic system, but of the damping characteristics of the mechanical system. The minimum time in which the final stress could be applied without overshoot was 0.02 seconds. Though any overshoot damped out quickly due to the feedback signal control, it produced significant effects both on the yield delay time (considerable reduction) and the preyield microcreep rate (considerable increase). Since the time resolution of the recorded data is of the order of 0.001 seconds the time to final load can be accurately accounted for in experiments where this time is significant in relation to the yield delay time.

Yield delay data were taken in tantalum at -20°F , 73°F , 200°F , and 400°F , and in columbium at -97°F , -20°F , 73°F , and 150°F . At the highest operating temperature in each set it was difficult to obtain reliable data. Only those which showed a reasonable functional dependence on stress are presented. Figure 9 through 12 show the summarised results of the various yield delay experiments.

Figure 6 demonstrates a typical yield delay recovery experiment. Each

complete set of such experiments was programmed to consist of the following steps.

- 1) A stress level was chosen from the yield delay information which was expected to lead to a reasonably long time to yield (e.g., from Figure 10 it can be seen that the 28,800 PSI used in the sample experiment should lead to a yield delay time of approximately 55 seconds at -20° F).

This stress level was applied rapidly and maintained constant for a preselected period of time less than the yield delay time.

The stress was removed rapidly and reapplied after a specified recovery time. This cycle was continued until macroscopic yield was definitely established.

- 2) Next, using the same stress level, the recovery time was varied with the objective of finding the recovery time which was just sufficient to provide complete recovery. The degree of recovery revealed itself by the number of cycles, that is total time at load, to which a specimen could be exposed until macroscopic yield occurred.
- 3) The same procedure was repeated with the same stress levels and a new series of recovery times but, during the recovery times, the specimen temperature was increased above the load cycle temperature (-20° F in the sample case). From the relative recovery times at two to three recovery temperatures the activation energy for recovery was to be calculated.

This technique, though basically sound, had several shortcomings.

Since relatively low stress levels must be used to allow sufficient time for observations (1 second was felt to be a minimum) the resulting anelastic microstrain was very small.

More serious, however, proved to be the thermal lag of the specimen which was quite large. It was enhanced by the thermal mass of the gripping mechanism, and, during low temperature experiments, by the excellent heat transfer to the cooling medium. As a result during large portions of the recovery time the specimen was not in thermal equilibrium. Of course, the higher the recovery temperature, the shorter will be the overall recovery time. Therefore it was difficult to establish an exact time-temperature relation during this period.

Without the latter shortcoming it would have been possible to theoretically predict the approximate recovery times at each temperature level from the initial experiment. Under the conditions described this was naturally impossible. Therefore, it was also economically unfeasible to carry out a complete set of experiments on a trial and error basis for several stress levels and the corresponding load cycle temperatures. Each specific experiment required, of course, the use of a different specimen.

Other difficulties, such as the provision of step function load cycling

and masking of strain recovery by thermal expansion, were easily overcome thanks to the quality of the experimental equipment on hand. Therefore, despite the fact that the final objective, determination of activation energies of the recovery process, could not be obtained, the yield delay recovery data still yielded some informative, though qualitative results.

RESULTS AND INTERPRETATIONS

As stated previously, the constant load (or stress) rate data were not utilized to investigate the anelastic behavior but served only to establish, with a minimum of experimental points, the stress and temperature conditions under which observable yield delay could be expected.

Figures 7 and 8 show the results both for tantalum and columbium. The straight lines represent the best linear fit of the data points at each experimental temperature based on a minimum of the RMS deviations. The elastic limit was in all cases identified with the yield point. On comparison with Figures 9 and 10 it can be seen that the times to yield were in general larger in the load rate test for a given final (or yield) stress than for the yield delay experiments. This was not in accordance with previous work with bcc metals ⁽⁸⁾, but would, in general, be expected from theory since the average applied stress during the load rate experiment is only half that of the yield stress.

Figure 7 STRESS RATE DEPENDENCE IN RECRYSTALLIZED TANTALUM
(RATE CONSTANT TO YIELD)

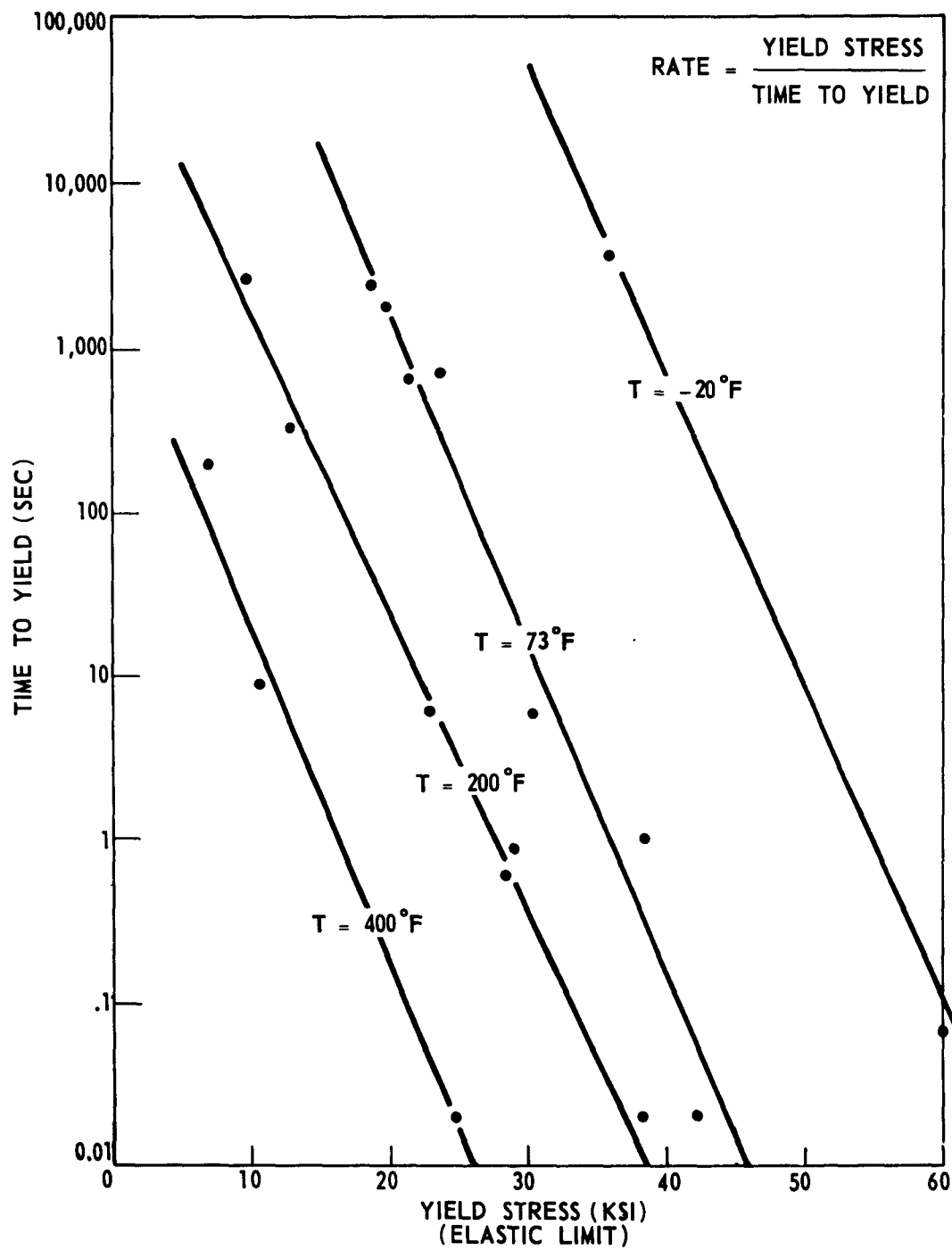


**Figure 8 STRESS RATE DEPENDENCE OF RECRYSTALLIZED COLUMBIUM
(RATE CONSTANT TO YIELD)**

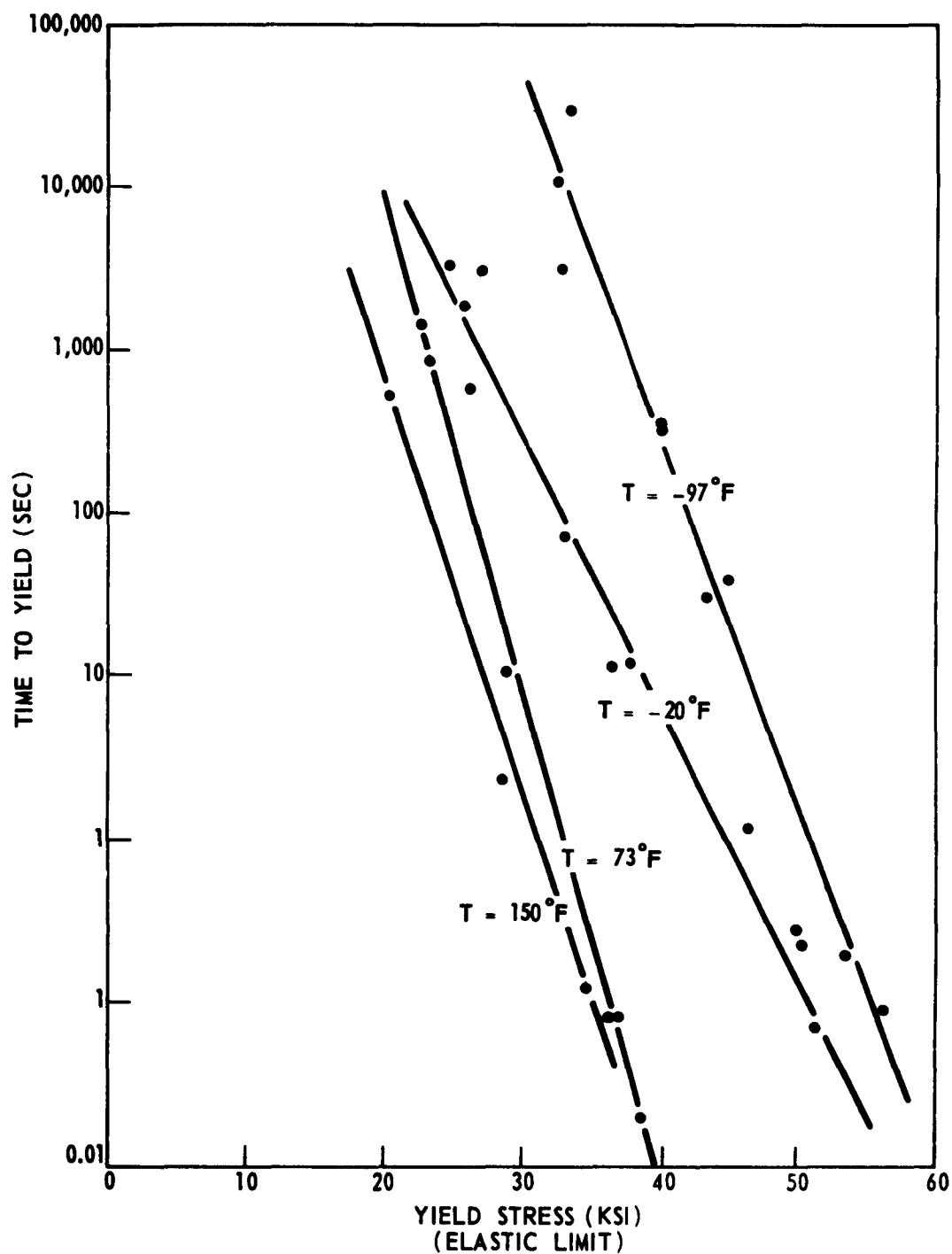


Figure 9 YIELD DELAY IN RECRYSTALLIZED TANTALUM

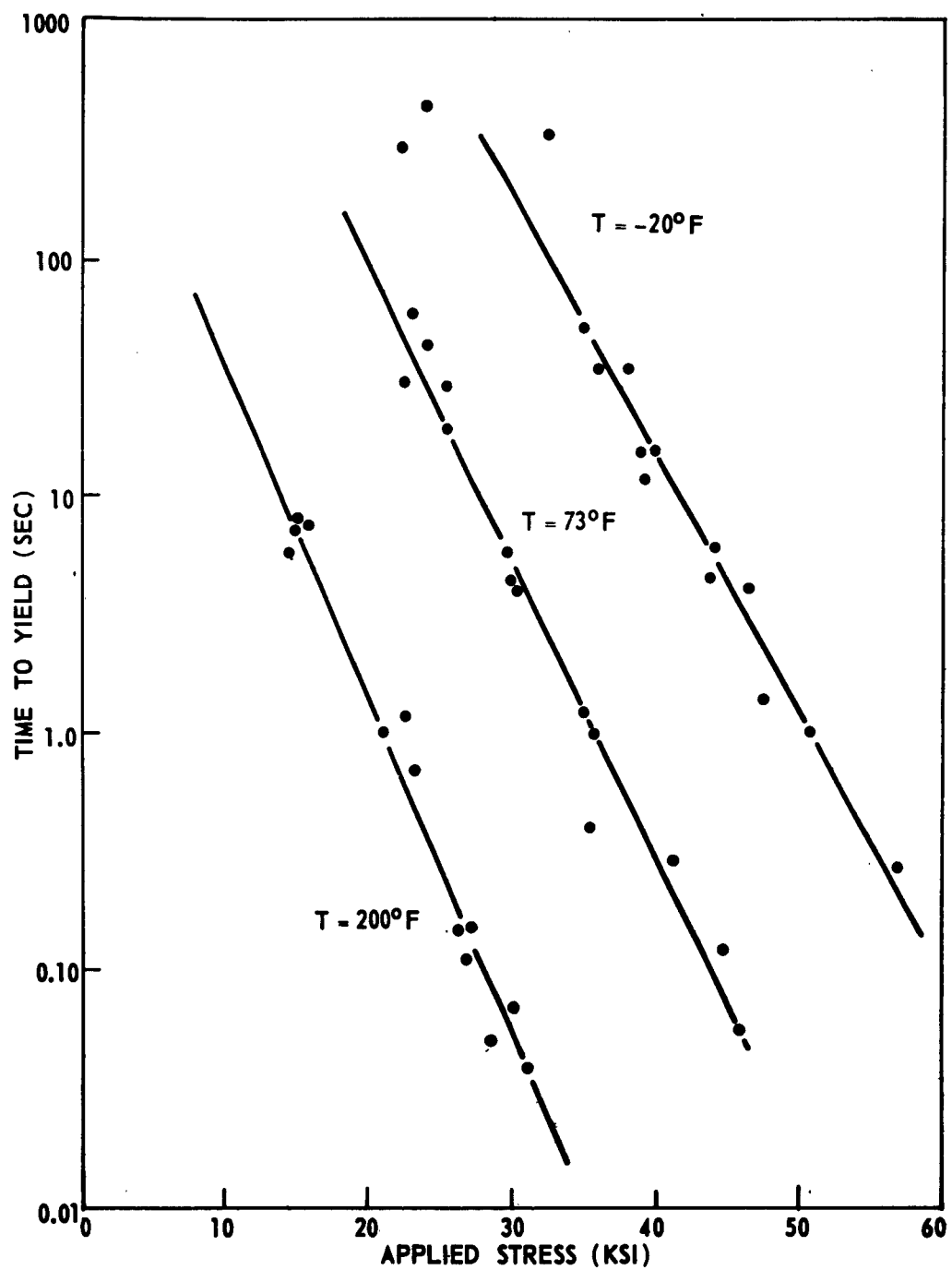


Figure 10 YIELD DELAY IN RECRYSTALLIZED COLUMBIUM

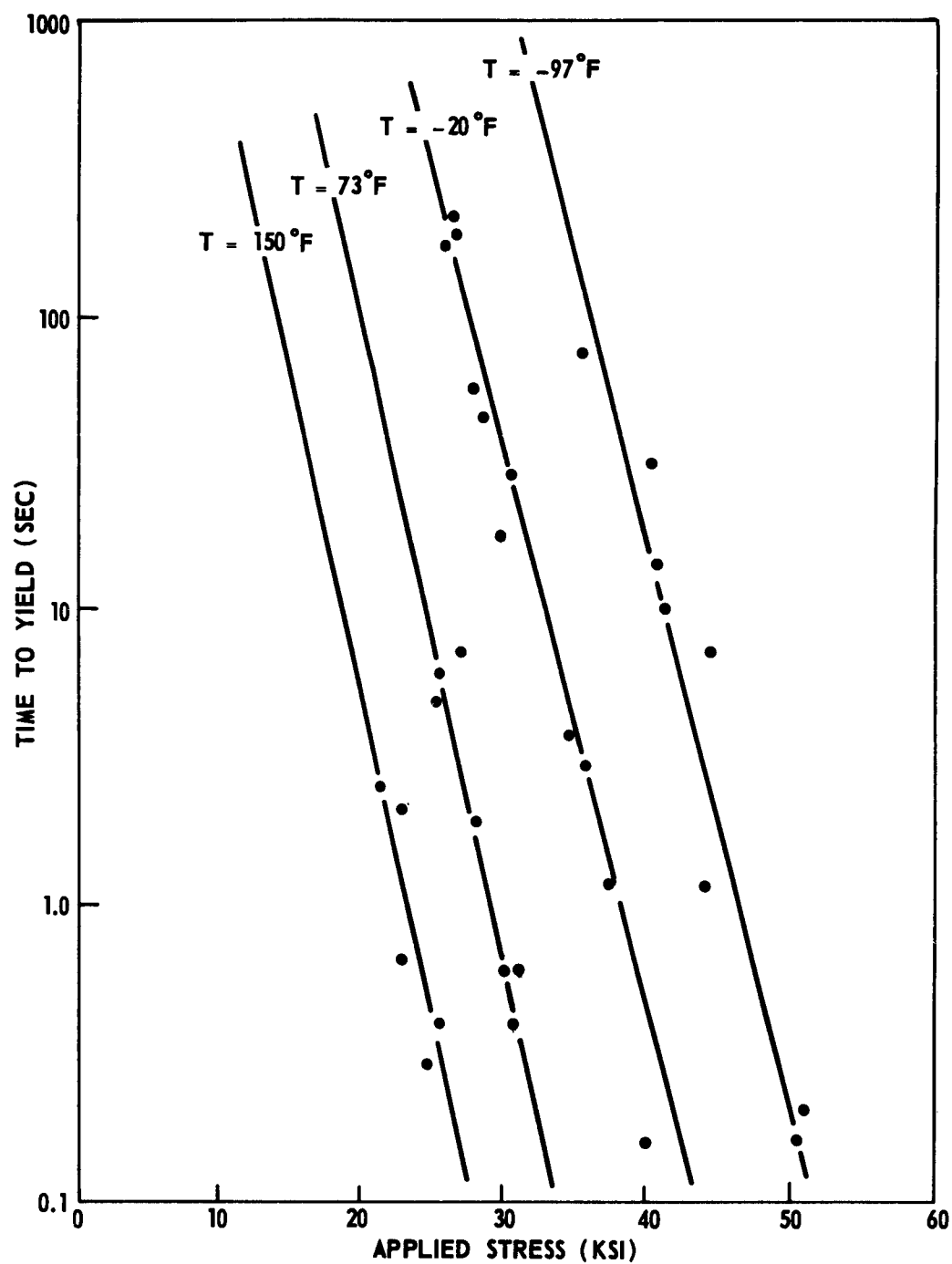


Figure 11 LINEAR MICROSTRAIN RATE IN RECRYSTALLIZED TANTALUM

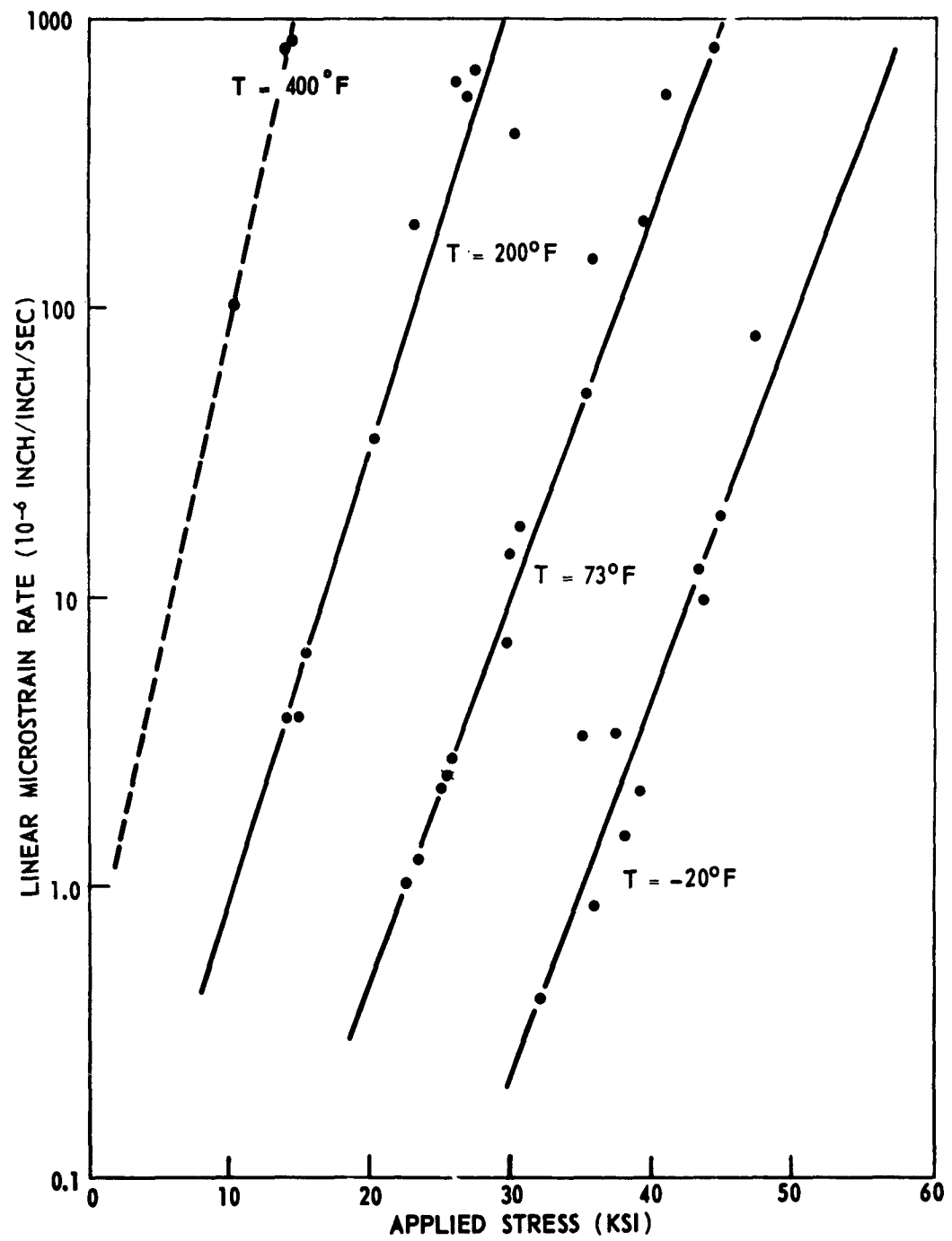
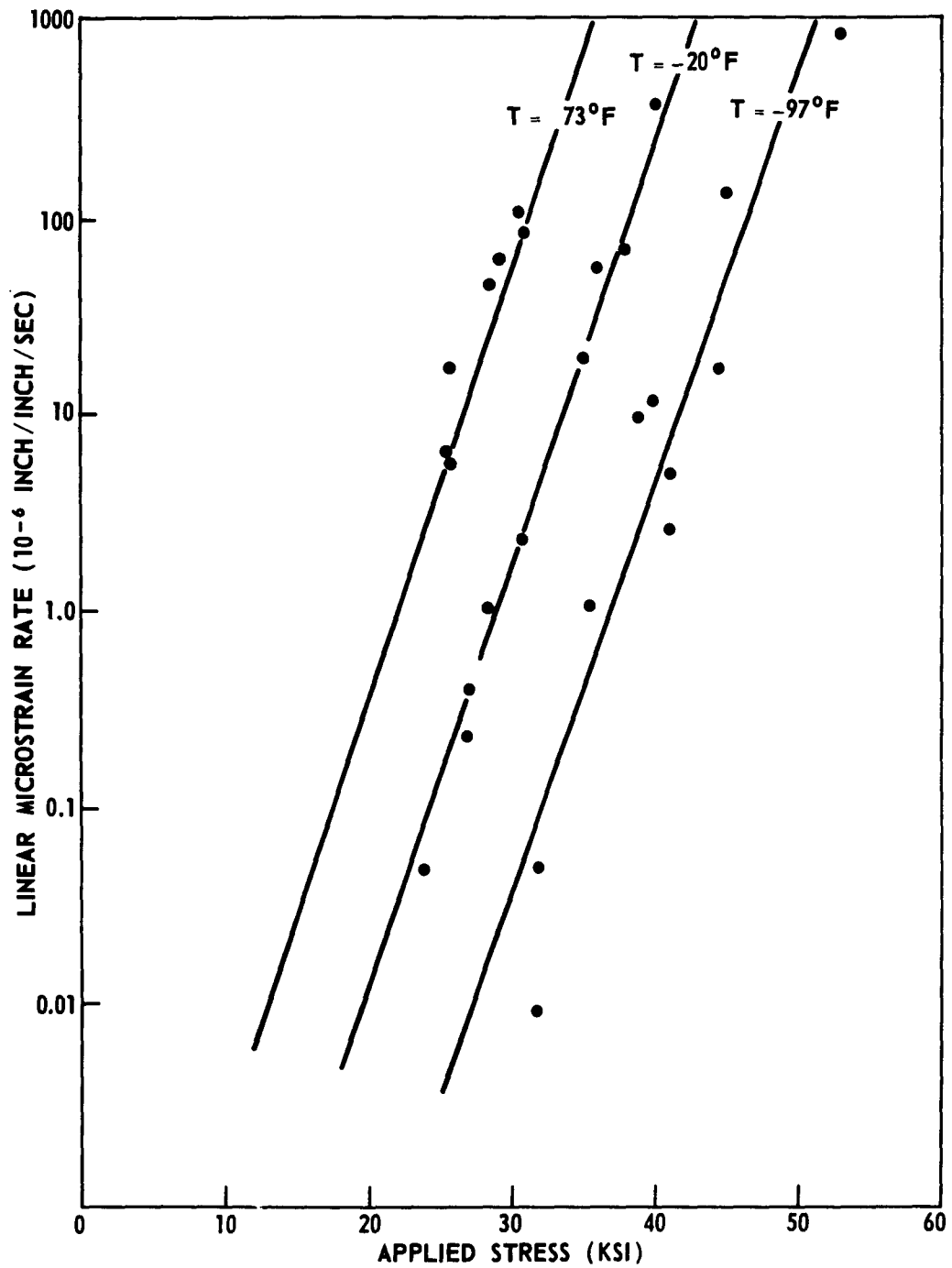


Figure 12 LINEAR MICROSTRAIN RATE IN RECRYSTALLIZED COLUMBIUM



Figures 7 and 8 show clearly that yield delay experiments below room temperature were required to obtain a reasonable coverage both with respect to temperatures and yield delay times. The experimental program which was originally scheduled to be performed entirely above room temperature was accordingly redirected.

The significant, experimental results of this study are contained in the strainrate and yield delay data presented in Figures 9 through 12. Within the limits of the experimental scatter, these data substantiate the dislocation - interstitial interaction model developed in the theoretical background section. Before discussing the implications of these results the reduction methods should be considered.

The microstrain rates quoted represent the initial, constant rates. This eliminated the time dependency which would not permit meaningful comparison of strain rates under the various stress-temperature conditions. Equations (11) and (A20) predict the constant, initial strain rate which was observed in all yield delay experiments, except in those where the time to yield was so short that the constant rate was masked by system damping (see initial 0.05 seconds in Figure 5). Data with the latter characteristics had to be neglected. This was minimized by adjusting the damping characteristics to the anticipated length of the experiment.

The yield point or time to yield was identified, as in Figure 5, with a

significant, continuous increase in slope. As our model predicts, the slope will normally decline after the constancy of the initial micro-strain rates rate ceases. This decline was observed prior to yield in many experiments. In several instances more than one slope was observed prior to macroscopic yield. Such changes in slope were not identified with the yield point since they were not continuously increasing. They were apparently caused by multiple contributors to the yield delay mechanism.

In very short yield delay experiments, compensation was made for the time to final load in establishing the yield delay time.

Several experimental data points had to be neglected because anomalous temperature effects were observed. This was the case when the highest rates of loading were applied in experiments of short duration. Under such loading conditions the temperature of the specimen would increase up to 2 to 3° F. Consequently, during the initial portion of the experiment, after the load was applied, a reduction in strain was observed which constituted the recovery of the thermal expansion. This reduction in strain was at first rather mysterious and temperature variations were not suspected since theory predicts adiabatic cooling during rapid elongation of metal. However it was then decided to mount thermocouples on the specimens and record the temperature history. The changes in temperature were clearly observed and the magnitude of the recorded strain corresponded to the expected thermal expansion. No attempt was made at this time to interpret

this phenomenon. The recovery times were, as expected for thermal processes, rather large. Since the observed thermal expansion was also of the same order of magnitude as the anelastic strain it presented a rather undesirable masking effect. It may be noted however that in most cases the effect became negligible if the loading time was changed from the minimum of 0.02 seconds to about 0.04 seconds. This presented in most cases no serious handicap. Careful inspection of Figure 5 shows the very slight remaining increase in temperature during loading at the slower rate.

On evaluating the data of all yield delay experiments it may first be noted that the stress dependency of the logarithm of both the yield delay time and the micro strain rate is relatively temperature insensitive. This follows the prediction made by Equation (7) which states that

$$\lambda_T = C \phi(\sigma) = C \sigma e^{\frac{l}{RT} - \beta \sigma} \quad (7a)$$

and by the corresponding expressions for the yield delay time and the anelastic strain rate in Equations (10) and (11). To illustrate, the anticipated variation in the slopes of strain rate versus applied stress in Figure 11 may be estimated as follows:

$$S = \frac{\partial \ln \dot{\epsilon}}{\partial \sigma} = \beta + \frac{l}{RT} + \frac{1}{\sigma} \quad (17)$$

Therefore,

$$\frac{\partial S}{\partial (1/T)} = \frac{l}{R}$$

$$\text{or } \Delta S = \frac{\ell}{R} \Delta\left(\frac{1}{T}\right)$$

Assuming an empirical value of 1.7×10^{-2} cal/mole/PSI (Appendix B) for ℓ in tantalum, it can be seen that the total change in slope over the temperature range of primary interest (-20° F to 200° F) is at most 1.16×10^{-5} , or at most a few percent of the slopes indicated in Figure 11. The value of ℓ used in this estimate is probably too large. Theoretical calculations (see Appendix B) indicate a much lower value in a strained lattice which has not reached martensitic phase equilibrium. It is obvious, that the experimental scatter of the data will not reveal such small deviations in slope.

It is also very doubtful that yield delay experiments can ever be utilized to better define the value of ℓ . The temperature ranges over which a single yield delay mechanism is prominent are relatively small and the behavior of real materials, particularly polycrystalline metals, will always lead to a certain amount of experimental scatter.

A more significant effect is anticipated from the more firmly established $1/\sigma$ term in Equation (17). Experimental scatter rules out correcting any one set of data for this term, because the total variation at any one temperature is more than one order of magnitude smaller due to the limited stress range. However, considering the average stress levels in each set (i.e., each experimental temperature) the average slopes may be corrected. It can be seen that this to some extent accounts for the apparently consistent increase in slopes with temperature.

Neglecting the temperature effect introduced by the term $l / R T$ we can calculate the following values for β from Equation (17) and the applicable figures.

<u>Metal</u>	<u>Temperature ° F</u>	<u>Type of data</u>	<u>Avg. Stress(KSI)</u>	<u>S(KSI⁻¹)</u>	<u>β(KSI⁻¹)</u>
Ta	-20	time to yield	42.3	.267	.243
Ta	73	time to yield	30.5	.289	.256
Ta	200	time to yield	22.9	.329	.285
Ta	-20	Microstrain rate	40.1	.306	.281
Ta	73	Microstrain rate	31.4	.317	.285
Ta	200	Microstrain rate	22.1	.363	.318
Cb	-97	time to yield	43.6	.435	.403
Cb	-20	time to yield	31.9	.439	.408
Cb	73	time to yield	28.2	.465	.430
Cb	150	time to yield	23.8	.492	.450
Cb	-97	Microstrain rate	40.0	.501	.472
Cb	-20	Microstrain rate	31.6	.508	.472
Cb	73	Microstrain rate	27.8	.512	.472

The values of β are in reasonable agreement with those calculated in Appendix C, considering the uncertainties in the definition of A. Two characteristics must be noted. Despite the corrections introduced by the average $1 / \sigma$ term, there is still a tendency for β to increase with temperature. Consideration was given to the fact that β is inversely proportional to the

shear modulus. However, the change in shear modulus is only about one percent over the range of interest and, therefore, not significant in these first order calculations. Consideration should however be given, as in the evaluation of the effective activation energies, that at higher temperatures different interstitials are likely to participate in the dislocation - interstitial interaction which controls β .

The second characteristic of interest is the apparently lower values of β when interpreted from the time to yield information. A difference must be anticipated from the theoretical model.

As stated repeatedly, the strain rate data are taken during the initial portion of the experiment where they are independent of time. The time to yield experiment allow no such assumption and from Equations (7) and

(1) it can be seen that

$$S = \frac{\partial \ln t_y}{\partial \sigma} = - \left[\beta + \frac{1}{\sigma} + \frac{\frac{\partial}{\partial \sigma} e^{-\lambda_I t_y}}{(1 - e^{-\lambda_I t_y})} \right]$$

$$= - \left[\beta + \frac{1}{\sigma} - \left(\beta \lambda_I t_y + \frac{1}{\sigma} \right) \frac{e^{-\lambda_I t_y}}{1 - e^{-\lambda_I t_y}} \right] \quad (18)$$

if ℓ/RT as well as any stress dependence in λ_D is neglected.

A simple solution of Equation (18) for β is not possible, but the equation indicates why β should be smaller when calculated from Equation (17) as was done for simplicity in the tabulated data.

Of particular interest are the activation energies resulting from the data in Figures 9 through 12. It has already been established that only effective activation energies can be deduced from the experimental data. Equation (16) makes it quite clear that without extensive iteration, since $\lambda_i = \lambda(Q_i)$, and without precise knowledge of the weight factors, ω_i , of each participating mechanism, it is not possible to establish the activation energy of each mechanism exactly.

Based on the straight line relationships, indicated in each set of data which were established by the statistical method of the least squares, the following activation energies were determined:

Metal	Temperature range	Type of data	Q_{eff} (cal/mole)
Ta	-20° F to 73° F	time to yield	10850
Ta	73° F to 200° F	time to yield	14200
Ta	-20° F to 73° F	micro strain rate	10550
Ta	73° F to 200° F	micro strain rate	14900
Ta	200° F to 400° F	micro strain rate	16700
Cb	-97° F to -20° F	time to yield	8625
Cb	-20° F to 73° F	time to yield	11350
Cb	73° F to 150° F	time to yield	13900
Cb	-97° F to -20° F	micro strain rate	9440
Cb	-20° F to 73° F	micro strain rate	10900

The activation energies were determined by the $\Delta\left(\frac{1}{T}\right)$ relation at identical stress levels, thus eliminating the effects of $\ln\sigma$ and $\beta\sigma$. There is, of course, the effect of the $\ell\sigma$ term which may increase the values a maximum of 600 cal/mole for the lowest value of Q tantalum, and a maximum of 700 cal/mole for the lowest value of Q columbium. These estimated maxima are again based on the conservatively high values of ℓ from empirical martensitic information (Appendix C).

Despite all the uncertainties as to the actual activation energies of the mechanism or mechanisms producing anelasticity in each temperature range, the data seem to clearly indicate that:

- 1) both the time to yield and the preyield microstrain rate are influenced by identical control mechanisms.
- 2) interstitial diffusion of hydrogen is a major contributor to the anelastic behavior, and, as the experimental temperatures increase contributors with high activation energies are apparently increasingly effective.

The activation energy for hydrogen diffusion in columbium has been fairly well established as being 9300 ± 600 cal/mol ⁽²³⁾. It is anticipated that the activation energy of hydrogen diffusion in tantalum is of approximately the same magnitude due to the similarity of the two metals and the similarity of the activation energies for other interstitials (usually slightly higher in tantalum - e.g., C and N).

There is a number of other solute elements in tantalum and columbium which are capable of increasing the effective activation energies with increasing

temperatures. These may conceivably be boron, silicon, and oxygen in the temperature range of interest.

Boron activation energies have been measured, with limited reliability, as 16900 ± 6100 cal/mole in tantalum and 14300 ± 5400 cal/mole in columbium⁽²⁴⁾. The chemical analysis of the experimental materials shows that apparently relatively small amounts of boron are present.

Silicon is a substitutional solute; however, its relatively large misfit of approximately 18%, should give a tendency to preferential ordering in a strained lattice and permit dislocation locking in the positive stress field of the dislocations. The activation energies for silicon have been measured, with the same limited degree of reliability as in the case of boron, as being approximately 11720 cal/mole in columbium and 6040 cal/mole in tantalum⁽²⁵⁾. These latter values may probably deviate by several thousand calories per mole. Considerable quantities of silicon are present in the experimental materials.

More reliable data are available for the activation energy of oxygen. Several sources⁽²⁶⁾ report values of approximately 26000 cal/mole in both metals. Deviations are of the order of several hundred calories per mole. The latter activation energy is quite high compared to that of hydrogen or the measured activation energies. However, the time, temperature and stress dependence of the effective activation energy, as shown in Equation (16), does not preclude the participation of oxygen in the

anelastic processes above room temperature. Without stress effects the relaxation time of oxygen in tantalum and columbium is of the order of 1 second near 400° F.

As indicated earlier the yield delay recovery experiments did not yield quantitatively useful data. However the following qualitative observations may be related.

In all experiments of this type the total time at load prior to macroscopic yield exceeded the time to yield in normal yield delay experiments when identical stresses and temperatures were employed. There was, however, little consistency with respect to the length of recovery time which was varied from 5 minutes to 30 minutes.

Although significant recovery of strains could not be observed if the recovery took place at the same temperature as applied during the load cycle, such recovery could be observed if the temperatures were raised some 200° F during recovery. This indicates, as expected from the theoretical model, that the relaxation times of the reorientation process are considerably larger without than with an applied stress. It was possible to obtain complete recovery in some cases which permitted load cycling of the specimens for many hours without yielding. In these cases the equivalent of two load cycles would have been sufficient to yield the specimens without recovery.

X-RAY DIFFRACTION MEASUREMENTS OF MICROSTRAIN

DISCUSSION

The proposed model of anelasticity implies diffusion induced reorientation of interstitials during the pre-yield deformation (micro-creep) of bcc refractory metals. If this is the case, one obvious result should be a change in lattice constant during the yield delay time and a recoverability of the lattice deformation by removing the applied load. It was felt, therefore, that x-ray diffraction measurements of lattice constants under the appropriate load conditions should give rather conclusive proof whether the pre-yield microstrain is merely the result of a limited number of dislocations propagating along slip planes or whether interstitials are significantly contributing to the microstrain.

It was realized from the beginning that it is rather ambitious to attempt a measurement of the interstitial induced lattice deformation. From experimental data it is known that the externally measured strain during microcreep was limited to at best a few hundreds micro inches per inch in the high purity materials under investigation. Also, the x-ray diffraction information was sensed in a Geiger counter assembly. This requires relatively long counting times if sensitivity is not to be sacrificed. Consequently experiments had to be carried out under conditions producing long yield delay times. As all applicable data or theories indicate, this meant operation at relatively low stress levels. This in turn requires operation at low anelastic strains (equilibrium distribution of

interstitials is a function of applied stress - see Appendix A). Fortunately, the resolution limit of the x-ray equipment at our disposal was higher than average and permitted observations with a sensitivity of better than ± 0.0001 Angstrom . This corresponds to a microstrain sensitivity limit of the order of 30 micro inches/inch.

Another factor that contributes to rather satisfactory results is that the lattice strains measured by x-ray diffraction are always larger than the externally measured strains in a corresponding direction if the lattice deformation represents a major portion of this strain. The external observations represent an average of the local strains which may vary from zero in grains whose crystal structure is such that the (111) plane is parallel to the direction of the applied tensile or compression stress (no preferred positions created), to a maximum in those grains where the cube edges of the unit cell are parallel to the applied stress. The x-ray diffraction measurements represent those of one set of planes only. For experimental expediency, i.e., to obtain maximum sensitivity, the plane chosen for x-ray observation is normally the one which produces maximum deformation, and maximum intensity from the diffracted radiation.

A verification of the occurrence of lattice deformation during microcreep has been definitely established from the consistent, repeatable trends of the observations both during the load and recovery cycle. It cannot be pretended, however, that the data have the accuracy implied in terms of

absolute magnitudes. However, the sensitivity is such that relative changes, which include the recovery information, are measured with the precision indicated in the data.

EXPERIMENTAL TECHNIQUES

It was anticipated to use only materials of the same constituency and with the same heat treatment as those used in the other yield delay experiments. However, columbium in the available purity did not lend itself very readily to reliable x-ray diffraction studies. This material showed anelastic micro strains of the order of 10 to 30 micro inches per inch only on application of the relatively low stresses required for long delay times (i.e., near the lower limit at which eventual yield was observed). This is not consistent with the sensitivity limits of the x-ray diffraction technique. Consequently, after experimental verification of the columbium behavior, it was decided to use molybdenum as an additional experimental material. This was to aid in the generalization of the observations to bcc metals. It was known from earlier experiments that in the arc-cast, recrystallized molybdenum on hand anelastic microstrains up to 400 micro inches per inch could be anticipated. Interstitial constituents in this material are, by weight, 0.013% C, 0.0007% O, 0.00011% N, and 0.00015% H.

A Norelco Geiger-counter diffractometer was used for measuring the lattice spacings, utilizing the 1.54050 Å radiation of the Cu K-alpha line. Data

were taken both in the (200) and (211) planes which are parallel or nearly parallel to the applied tensile stress direction. Obviously, it was not practical to measure the lattice deformation in the direction of stress. Consequently, the observed lattice deformations and the externally measured strain had opposite signs and were compared to one another, in a macroscopic sense, by introducing a transformation factor on the order of Poisson's ratio. It is shown in Appendix D, that this transformation factor for interstitial anelastic strains is always less than Poisson's ratio. Both planes used yield relatively high Bragg angles. This yields the greatest sensitivity in the particular x-ray diffraction unit used for this investigation. The initial set of data, with molybdenum as the sample material, was taken during the recovery mode only. Specimens were preloaded, as during yield delay experiment, for a period such that no yield occurred. The material was then unloaded, its remaining strain measured, and mounted into the x-ray diffractometer. Repeated measurements of lattice constants and externally observed strain were assumed indicative of the strain recovery. This worked reasonably well for molybdenum, even though it was impossible to obtain very accurate, absolute data. Despite the fact that various calibration runs were made with original and preloaded specimens, the accuracy was very much reduced by the lack of repeatability when mounting and remounting in specimens in the x-ray unit. While this did not take away from the recovery information in molybdenum it was a serious handicap to experiments in tantalum and columbium, where smaller anelastic strains are observed.

**Figure 13 X-RAY DIFFRACTION UNIT
(INCLUDING LOAD CELL FOR STRESSING SPECIMENS
DURING DIFFRACTION MEASUREMENTS)**



It was also highly desirable to observe the microstrain during the load as well as the recovery cycle. Therefore, a hydraulically controlled load unit was built which permitted the observation of lattice deformation while under load, (Figure 13). The unit requires the use of flat specimens whose dimensions need approximately be: 2.4 inches long, by .45 inches wide, by .05 inches thick. Suitable specimens were obtained from the same melt, with the same heat treatment, and the same (twice verified) constituency, as the tensile specimens used in the other experiments discussed in this report. Lattice constants were then measured prior to loading, during loading, and after unloading without having to change the position of the specimen.

As will be discussed later, recovery times are very much longer than the relaxation times of strain when under load. It was therefore necessary to build a heater for the specimens which was applied to the specimens between recovery measurements for controlled periods of time. The temperature was measured by a thermocouple mounted, with a strain gage, on the flat side of the specimen, opposite the side under observation. The strain gage measured the macroscopic strain, the anelastic strain, and served to prevent thermal expansion from yielding erroneous information.

RESULTS AND INTERPRETATION

The following tables summarize the results of various x-ray diffractometer experiments. Special conditions are either listed with each set of data or elaborated in the follow-on discussion of the results.

Set #1

Conditions: Specimens loaded to given stress and gage strain observed. Specimens unloaded and mounted in x-ray unit. Change in lattice strain observed. Heated to average of 100° C for 15 minutes. All strains normal to plane of observation.

Number	Material	Stress (PSI)	Anelastic Gage Strain (Micro inch/inch)	Anelastic Lattice Strain (Recovery) (Micro inch/inch)	Plane
1	Mo	55000 0	-396 ---	--- +508	200
2	Mo	55000 0	--- ---	--- +925	200
3	Mo	65000 0	-320 ---	--- 0*	200
4	Mo	55000 0	-32 ---	--- +190	200
5	Mo	55000 0	-32 ---	--- +63	200

* Material had yielded, recovery of lattice strain apparently occurred immediately on yield.
Sample was not heated during recovery.

Set #2

Conditions:

Specimens mounted in x-ray diffractometer; initial lattice constant measured, stress applied; initial and final lattice strains and gage strains observed; stress removed; initial and final gage & lattice strains observed during recovery. Recovery observed over periods up to 30 minutes. Heating applied only if no significant recovery occurred ($T = 100^\circ \text{C}$).

Number	Material	Stress (PSI)	Anelastic Gage Strain (Micro inch/inch)	Anelastic Lattice Strain (micro inch/inch)	Initial and Final Lattice Constant (\AA°)	Plane
6	Ta	21000 0	-3.5 +3.5	----- -----	1.3478 1.3478	211
7	Ta	23000 0	-52.5 +45.5	-180 +120	1.6505 1.6504	200
8	Ta	23000 0	-21.0 +7.0	-136 +75	1.3478 1.3478	211
9	Ta	23000 0	-40.25 +17.5	-120 +60	1.6502 1.6502	200 200
10	Mo	55000	-43.5 +32.0	-451 +322	(1.5492) (1.5490)	200
11	Mo	55000	-30.4 +19.2	-380 +190	----- -----	200
12	Cb.	21000 0	-3.8 +3.8	----- -----	1.3478 1.3478	211
13	Cb	23000 0	-23 +8	-150 +150	1.3478 1.3478	211
14	Cb	23000	-57 +11.4	-180 +120	1.6505 1.6504	200
15*	Ta	23000 0	-247 -1070 (remaining)	-121 +121	1.6512 1.6512	200

*Specimen yielded.

As stated previously, it is not realistic to evaluate quantitatively the absolute values presented in the data. It may be noted, however, that in all three sets of data the lattice strain information is quite consistent, in particular that obtained when the specimens were mounted in the load unit throughout the experiment. The gage measurements are apparently not quite as reliable. In these experiments SR-4 gages were used which are never quite satisfactory for cyclic loading or for intermittent measurements such as were necessary in Set #1. This is the reason that an induction type transducer is used for all other experiments. The use of such a device was not practical for the x-ray study.

Despite the rather unsatisfactory technique used to obtain the data in Set #1, the relative values are consistent with the anticipated trends. One of the reasons why the recovered lattice strains should be larger than the microstrain measured by strain gage during yield delay was discussed previously (single orientation versus average from random orientations). In all experiments but No. 5 complete recovery of the anelastic lattice strain was apparently achieved during the recovery period. That this lattice strain represents at least a very significant portion of the gross microstrain is obvious despite the uncertainty in the absolute values.

To recover the lattice strain in a reasonable time, heating was necessary. This could be anticipated. From previous experiments ⁽⁸⁾, it was established that the activation energy of the interstitial diffusion of C in

molybdenum with stresses of the order of 55000 psi applied was about $2/3$ that without stress. The relaxation time, being an exponential function of the activation energy (Q_c appx. 25000 cal/mole), becomes quite large when no stress is applied. Raising the temperature from 293° K to about 393° K will compensate for the effect of change in activation energy and produce observable recovery in a reasonable time.

In Set No. 2, the consistency of the initial and final lattice constant data provides a certain level of confidence in the improved technique used here and the resulting measurements of lattice strains. It appears again that more recovery was obtained than either of the strain measurements indicates. Apparently the delay necessitated to allow for a sufficiently large number of counts during each measurement affected the measurement to the extent that only partial recovery of the lattice strain was observed, (for example, experiments No. 8 and 9). The final value of the lattice constant implies that most of the anelastic lattice strain was recovered in each case. Only in experiments 8 and 10 was heat applied during the recovery. Again, this is consistent with the theory inasmuch as in tantalum and columbium the activation energies for the mechanism controlling micro creep, reduced to zero stress, is much lower than in molybdenum. Application of heat was probably not necessary in experiment No. 9. This experiment represented a rerun of No. 8 where the lattice strain recovery observed was relatively small. It was hoped that with temperature the recovery would be more complete. As stated above this

was more than likely caused by observation of the recovery during a limited time span rather than by incomplete recovery.

The absolute values of the lattice constants in Experiment No. 10 seem somewhat doubtful and are not in agreement with other, accepted data (about 1.57\AA).

Of some interest are the results of experiment No. 15. This specimen yielded during the experiment, and as can be seen complete recovery of the lattice strain occurred, while the gage strain indicated permanent plastic deformation.

This is apparently incompatible with the theory that microstrain prior to yield is caused exclusively by dislocations. However, additional and more carefully controlled experiments will be required to fully justify this argument.

In summarizing it may be stated, despite the sensitivity limited technique afforded by x-ray diffractometry, there is sufficient consistency in the results to state that microcreep during yield delay is accompanied by lattice strain such as would be expected if interstitial reorientation takes place. The magnitude of this lattice strain is such that it can account for all or at least a large portion of the microstrain observed externally by gage measurements. As is required by the interstitial diffusion model of pre-yield anelasticity, the lattice strain is, at least to a large degree, recoverable. Apparently, the recovery time is large

compared to the relaxation time of the pre-yield microcreep. This is apparently caused by the reduction of activation energy in the latter case due to the applied stress.

INTERNAL FRICTION STUDIES

DISCUSSION

In anticipation of significant contribution to the anelasticity of tantalum and columbium by interstitials such as oxygen, carbon and nitrogen it was thought desirable to determine the activation energies for diffusion (or relaxation times) of these constituents by internal friction techniques. There are well established data available on the internal friction peaks in question^(26 , 27). However, with the necessary facility readily available it was considered worthwhile to spot check the particular materials on hand for interaction effects and any other anomalies which could possibly result in an erroneous interpretation of the anelastic data from other experiments.

As was later established, the interstitials listed above produced only very minor contributions to the preyield anelastic behavior of the metals under investigation. The primary contribution apparently resulted from hydrogen diffusion and hydrogen dislocation interaction. Due to the low activation energies for these processes, the internal friction peaks can only be observed at relatively low temperatures (or very high frequencies). The apparatus on hand was primarily designed for high temperature operation and, therefore, is not applicable below room temperature. Also a high frequency limit is inherent in this device which is controlled by the

stiffness of the experimental material. Thus it was not feasible to study the internal friction peak of hydrogen and hydrogen-dislocation interaction. This makes the results described below somewhat academic for the present phase of the contract but still useful as reference information for future, high temperature studies.

EXPERIMENTAL TECHNIQUES

The internal friction of both tantalum and columbium was determined by measuring the decay time of a vibrating reed. The reed is electro statically excited to its resonance frequency, the driving force removed, and the amplitude decay recorded on a direct write, logarithmic time base recorder. Signal pickup is also obtained electrostatically, the specimen representing one electrode of an air gap capacitor.

The reed specimen, operating in a fixed-free mode is suspended vertically to prevent nonsymmetrical gravity effects. A tube furnace surrounds the specimen mount, the driving mechanism, and the pickup. In this arrangement the system is as nearly as possible in thermal equilibrium. The whole system is then immersed in a vacuum which prevents specimen oxidation as well as air damping effects.

Specimen temperature is controlled by a thermocouple near the specimen rather than on the specimen to eliminate another possible error in the

decay measurements due to external damping. This thermocouple was carefully calibrated against thermocouples mounted in three positions on a calibration specimen.

The specimen material was identical to that used in the other experiments, i.e., it came from the same melt and underwent identical heat treatment.

The nominal dimensions of the specimens were .40 inches wide by .05 inches thick by 7 inches in length. However, the apparatus is constructed so as to permit a variation of the effective length of the reed specimen prior to each experiment. This in turn provides the control over the desired resonance frequency of each specimen. The actual resonance frequency is monitored during experiments by an appropriate frequency meter.

The logarithmic time base recorder has the advantage that the decay is displayed over several decades (up to 25 db), thus increasing the accuracy of the observations. Any forced rather than natural frequency which may have been imposed on the specimen dampens out quickly and, with the available recording technique, sufficient data are available to permit the measurement of the decay at the natural frequency.

The linear data display which results from the logarithmic time base of the recorder is a great aid in the data reduction.

Efforts to utilize inert gases to prevent oxydation were discarded due to damping effects even at relatively low pressures and the low sparking potential of most inert gases.

The performance limitations of the apparatus, as it was originally developed, are the upper temperature limit which is somewhat higher than 1000° C and the lower temperature limit which is room temperature. No provisions are made for cooling.

The upper limit is set by the original vacuum system which cannot prevent oxidation of columbium and tantalum at higher temperatures and the thermal expansion of the system, which though considered in the design, causes problems in maintaining control over the small gap between the specimen and the driving and pickup electrodes. A careful balance must be maintained between these two gaps to obtain the necessary driving force, sufficient pickup and a specimen amplitude small enough to prevent sparking or short circuiting during vibration. The driving voltage is in the neighborhood of 1000 volt.

The frequency limitation of the system is primarily determined by the stiffness of the specimen material. The frequency or wave length is a function of the length of the specimen; the higher the frequency desired

the shorter must be the specimen. Without reduction in specimen width and thickness, the stiffness increases rapidly as the specimen is shortened and soon reaches the point where the electrostatic driving force is insufficient to produce measurable amplitudes. Mechanical impulse excitation was considered but not introduced because it would reduce the control over the vibration amplitude. This could have a severe effect on the decay measurements.

For future work, such as discussed in the last section of this report, a modified internal friction unit has been designed and is presently nearing completion.

RESULTS AND INTERPRETATION

Figures 14 through 17 show internal friction versus the inverse of temperature for pure, recrystallized tantalum and columbium. The frequencies noted on these figures correspond to those at which the major internal friction peaks occur. The frequencies, being the resonance frequency of the specimens, varied slightly with temperature (due to a change in elastic modulus). For example the resonance frequency for the data shown in Figure 14 varied from 68 cps at room temperature to 66 cps at 600° F.

There are a number of techniques for determining the activation energy of a process from internal friction data. The one chosen here is that of

**Figure 14 INTERNAL FRICTION IN RECRYSTALLIZED TANTALUM
(NOMINAL RESONANCE FREQUENCY 67 CPS)**

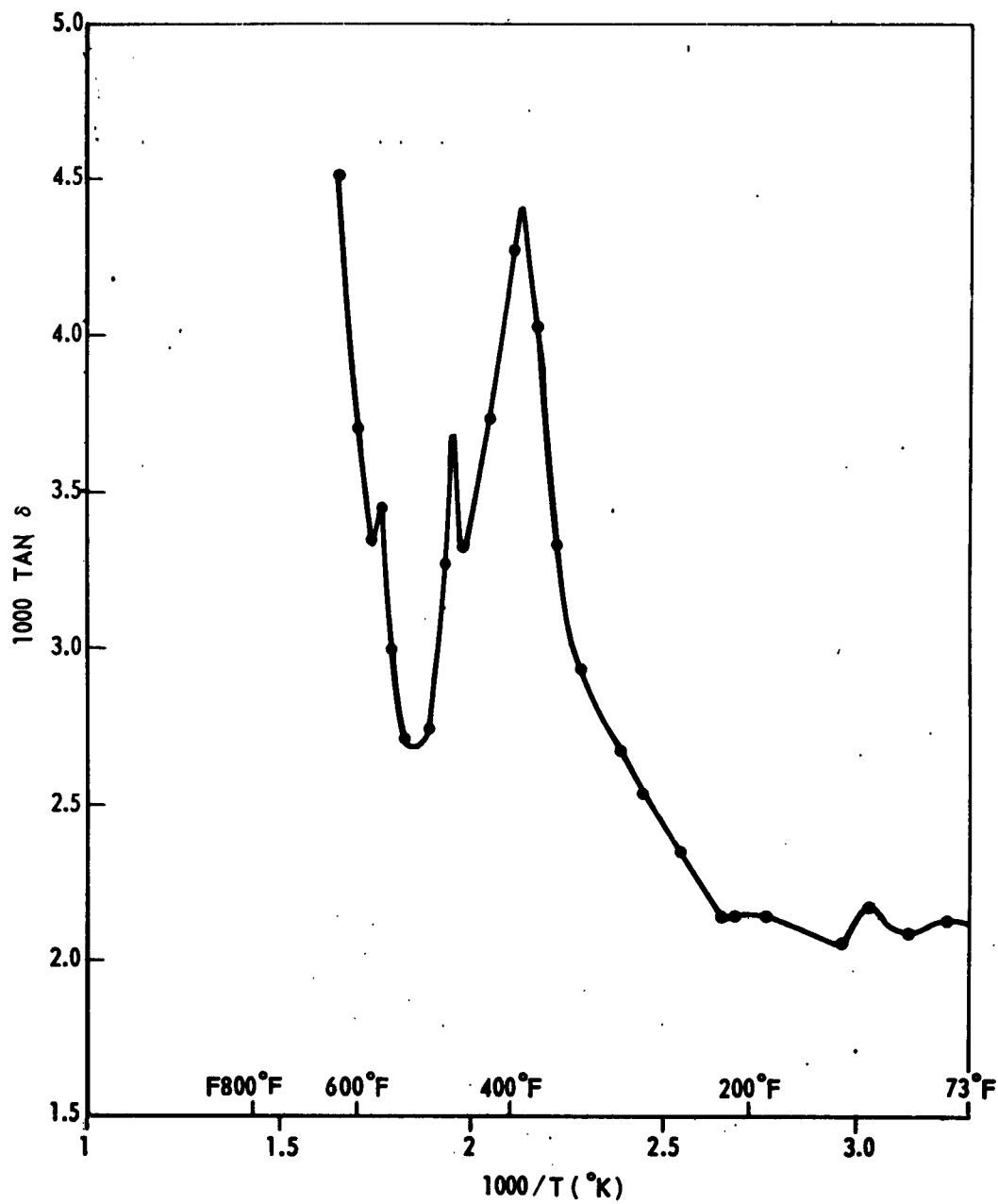


Figure 15 INTERNAL FRICTION IN RECRYSTALLIZED TANTALUM
(NOMINAL RESONANCE FREQUENCY 36 CPS)

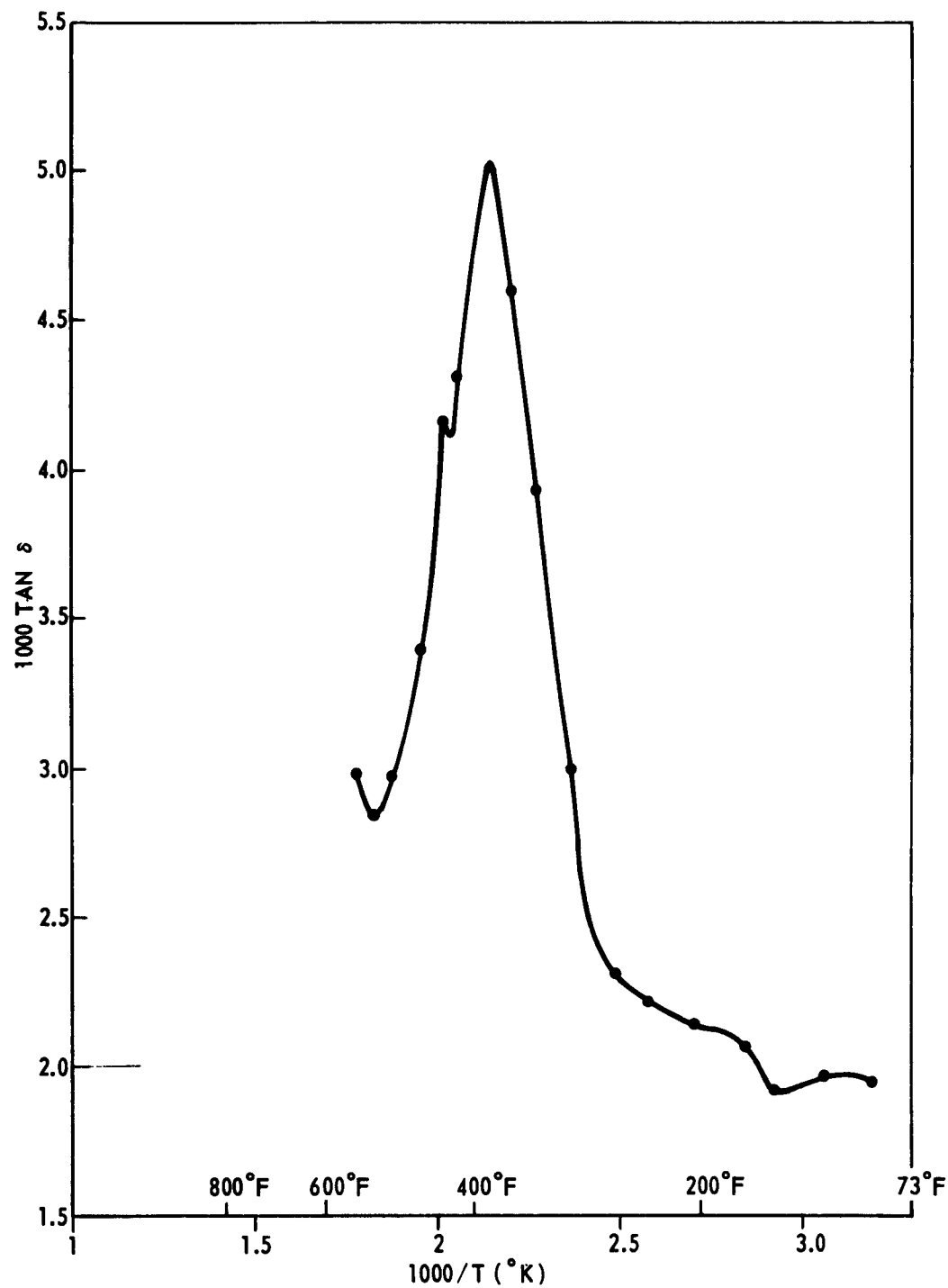
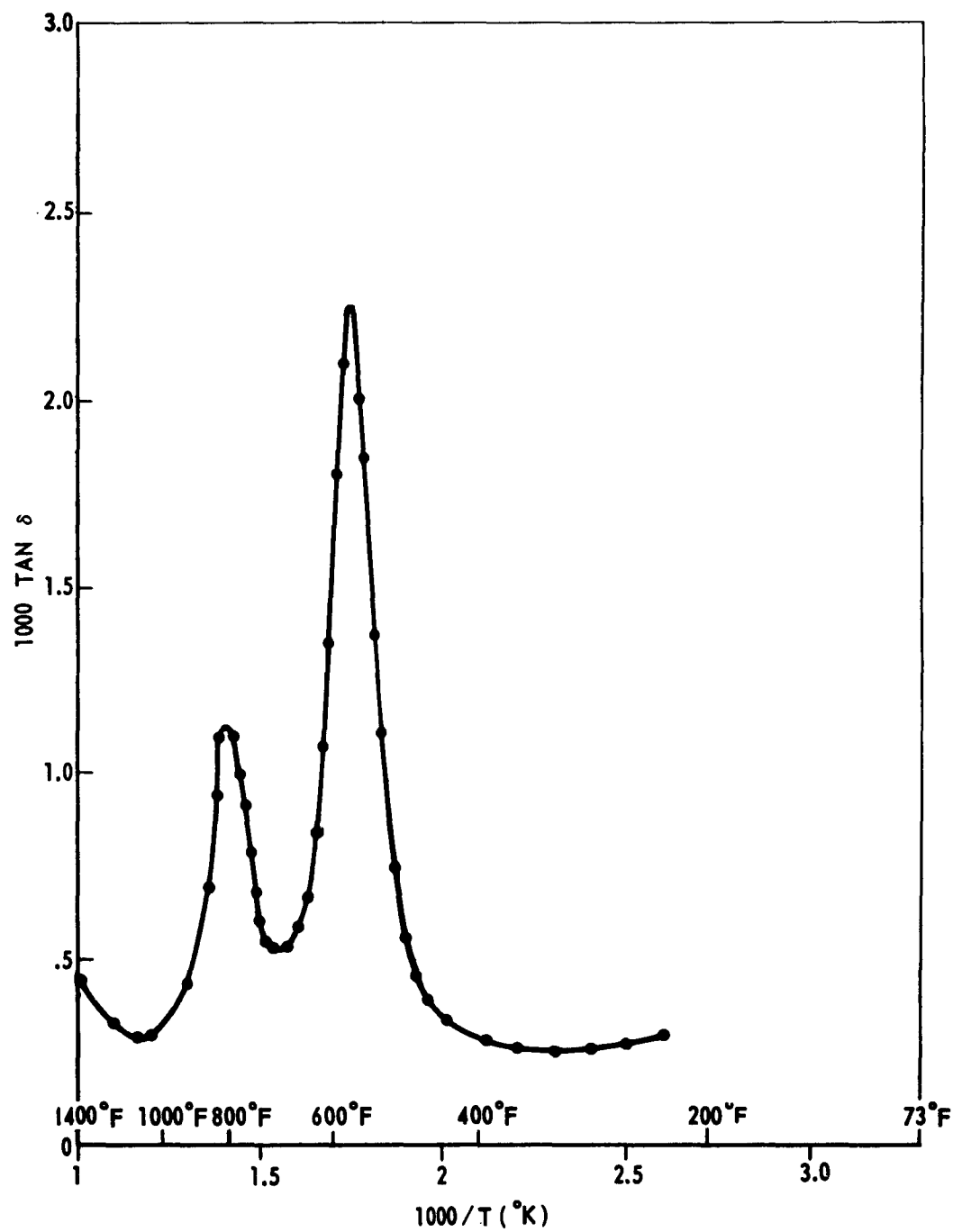
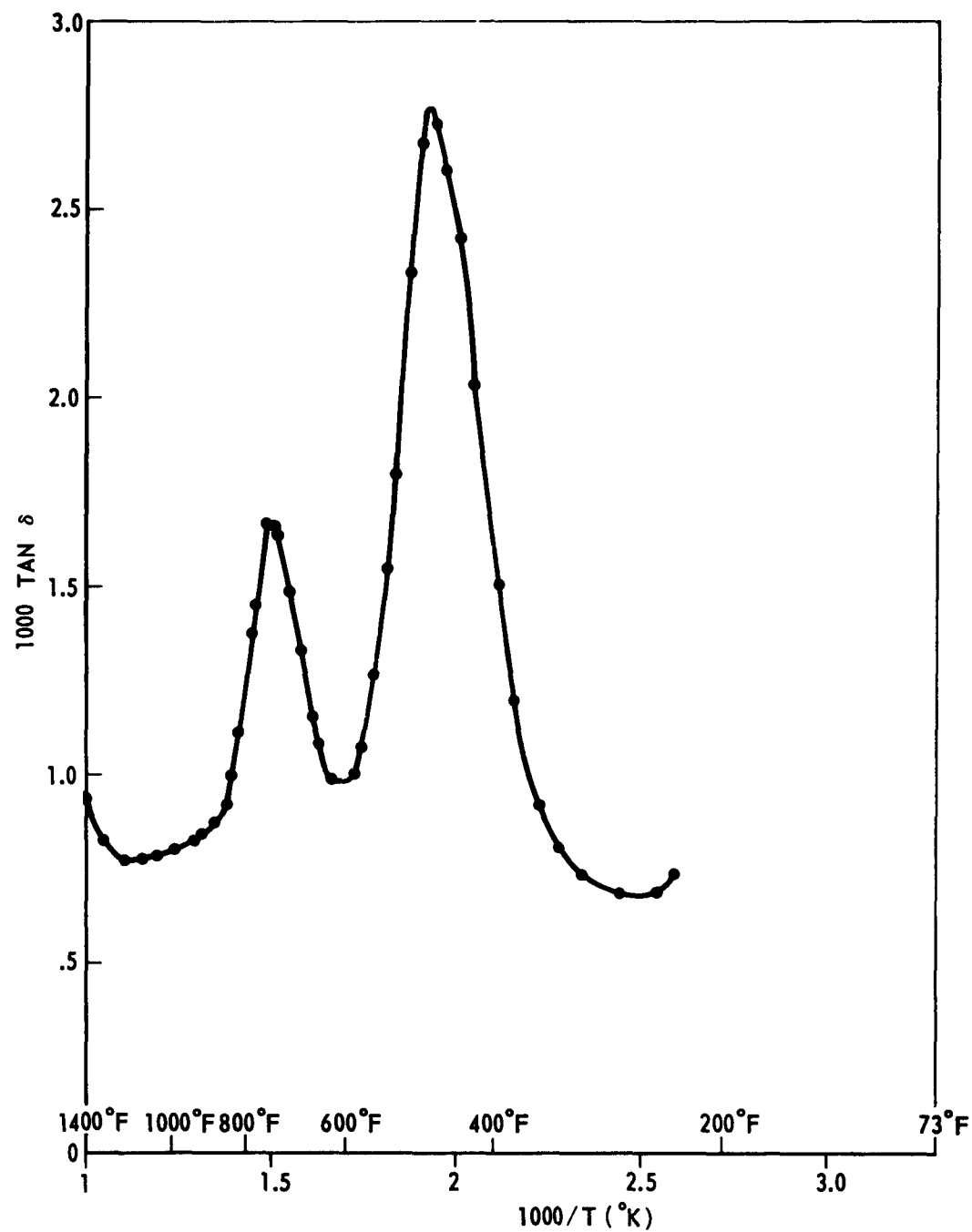


Figure 16 INTERNAL FRICTION IN RECRYSTALLIZED COLUMBIUM
(NOMINAL RESONANCE FREQUENCY 250 CPS)



**Figure 17 INTERNAL FRICTION IN RECRYSTALLIZED COLUMBIUM
(NOMINAL RESONANCE FREQUENCY 66 CPS)**



Wert and Marx⁽²⁸⁾, which is based on the equation

$$Q = RT \ln\left(\frac{\nu}{f_m}\right) + T \Delta S \quad (19)$$

In this equation ν is the atomic frequency and f_m the frequency at which maximum damping occurs in an experiment where the temperature is held constant and the frequency varied.

In our experimental approach, the frequency is held relatively constant and the temperature is varied. Therefore T is replaced in Equation (19) by T_m , the absolute temperature at which maximum damping occurs.

The greatest error is introduced by the uncertainty in the entropy. However this error is relatively small. The term $T \Delta S$ is usually less than 10% of the value of Q and ΔS can be calculated to a fair degree of accuracy from

$$\Delta S = Q \frac{\partial \mu / \mu_0}{\partial T} \left(\frac{\mu_{\text{elastic mod. at temp. } T}}{\mu_0_{\text{elastic mod. at ref. temp. } T_0}} \right)$$

Obviously some iteration is required to minimize any errors.

Equation (19) is also relatively insensitive to the location of T_m . The experimental accuracy used in this work, which was only considered a spotcheck approach, was sufficient to reduce possible errors to within a few hundred calories per mole.

A more precise relation for the evaluation of internal friction data was
(29)
derived by Zener and is of the form

$$R \ln (f_2/f_1) = Q (1/T_2 - 1/T_1) \quad (20)$$

Here the atomic frequency and the entropy do not enter into the evaluation. However, this equation is so sensitive to the location of T_m that with normal experimental procedures and consequent experimental errors, the reliability is not better than that obtained with Equation (19).

The following tables give the results of the internal friction measurements. The data were taken for two frequencies. This is not required by Equation (19) but serves to increase the reliability of the results. The atomic frequencies were calculated from rate theory for each temperature. The latest available data on the change of dynamic elastic modulus of tantalum and columbium were used to calculate the entropy.

<u>TANTALUM</u>						
	$f(\text{cps})$	$\frac{10^3}{T_m} (^{\circ}\text{K}^{-1})$	$\nu (10^{13} \text{cps})$	$\Delta S \left(\frac{\text{Cal}}{\text{Mole} \cdot ^{\circ}\text{K}} \right)$	$Q \left(\frac{\text{Cal}}{\text{Mole}} \right)$	Probable Source
1	67	2.13	.98	3.47	25742	oxygen
2	36	2.15	.97	3.47	26100	
<u>COLUMBIUM</u>						
1	66	1.93	1.06	3.16	28400	oxygen
2	250	1.75	1.19	3.16	29900	
3	66	1.49	1.39	4.10	37700	carbon and nitrogen
4	250	1.40	1.48	4.10	38400	

If it can be assumed that the entropy values are accurate to within ± 1 cal/mole/ $^{\circ}$ K a deviation of approximately ± 500 cal/mole results in the apparent activation energy of O in Ta and Nb; and a deviation of approximately ± 700 in the apparent activation energy of C and N in Nb. The maximum experimental error due to locating T_m results in a deviation of ± 300 cal/mole for the case of O in Nb at 66 cps.

The identification of the activation energies is based on the data by Powers and Doyle⁽²⁷⁾. The tantalum data agree quite well with those of Powers and Doyle. However, those for columbium are approximately 10% higher for both peaks observed. No theoretical or experimental explanation is readily available for this discrepancy.

It may also be noted that in Figure 14 the internal friction rises sharply again to the left of the apparent oxygen peak. This is to be expected inasmuch as the peak for N in Ta should occur at about $1.6 \times 10^{-3} (^{\circ}\text{K})^{-1}$ for an anticipated activation energy of approximately 37,500 cal/mole⁽²⁷⁾.

HIGH TEMPERATURE STUDIES

DISCUSSION

The work discussed in this section is of very preliminary nature. It represents the initial, exploratory phase of a program whose objective it is to establish the presence and causes for anelasticity in tantalum and columbium in a temperature range extending up to 3000° F. Though this program as such represents an extension of the work discussed in the previous section it is anticipated that entirely different mechanisms control the anelasticity in the high temperature region.

At this early date it appears not very useful to discuss phenomena resulting from anelasticity such as yield delay and, possibly, upper yield points. It is more appropriate to limit the considerations to anelasticity itself as defined basically by a phase difference between the stress and strain history of a material. It is for this reason that the initial emphasis of the experimental work will be on internal friction which is as powerful a tool for identifying anelasticity mechanisms as is spectroscopy in other fields of science. Careful internal friction measurements can reveal not only the contributors to the mechanism but also the manner in which they contribute.

To amplify on the statement that contributors other than interstitials are necessary to cause anelasticity at high temperatures it may be helpful to

consider a typical example. The relaxation time of the diffusion process of nitrogen in tantalum ($Q \cong 38000$ cal/mole) varies from approximately 10^{14} seconds at room temperature to 1 second near 400° F and 10^{-4} seconds near 1000° F. The relaxation times of hydrogen in tantalum, which appear to have such a significant effect on the anelasticity of tantalum near room temperature are orders of magnitude smaller than those of nitrogen. Obviously, at very high temperatures such interstitial contributions can barely be observed.

At these higher temperatures we can however suspect that mechanisms such as grain boundary viscosity, which appears very generally to have activation energies equivalent to those of self diffusion (of the order of 100,000 cal/mole in most bcc metals), and probably preferential diffusion of substitutional solute atoms of significant geometrical and electrical misfit, or pairs thereof, will have a marked effect on the anelasticity. Without referring to specific experimental values it can be said that the relaxation times of these latter mechanisms are from three to ten orders of magnitude larger than those of interstitial diffusion. This is nicely demonstrated in the illustrative relaxation spectrum presented by Zener. (29)

Of particular interest is the contribution made by grain boundaries. It was therefore decided to make this the first parameter of the high temperature relaxation spectrum analysis. At the high temperatures which are contemplated for the experimental program it may well be that significant

changes in grain size occur during the experimentation due to secondary grain growth (above the recrystallisation temperature). It is hoped that this will lead to additional interesting results. These may be of considerable practical value since very high temperature application is, to say the least, not uncommon for refractory metals.

To supplement or complement the internal friction data, simultaneous dynamic modulus measurements will be made.

Although the emphasis in the initial phases of the work will be on the relaxation spectrum as determined by internal friction, work has also started on the strain rate sensitivity of the materials under investigation with grain size and temperature being the experimental parameters. As in the case of the medium temperature studies this will permit an early exploration of temperature ranges where such phenomena as yield delay can be reasonably expected to be observed. It is again anticipated that the time to yield under various strain rate conditions is at least indicative of the yield delay time that may be expected if a stress, equivalent to the yield stress for a particular strain rate, is applied very rapidly and maintained constant.

The strain rate experiments will also yield strain rate coefficients as a function of temperature and grain size. These strain rate coefficients, much like internal friction data, will provide additional information on apparent relaxation peaks.

EXPERIMENTAL TECHNIQUES

During the initial portion of the high temperature study the tensile and internal friction equipment was redesigned and modified as required for high temperature work with pure refractory metals.

The tensile unit as described in a previous section has all provisions for high temperature operation. However in this specialized research effort it was mandatory that any oxidation of the specimens be prevented. To this end the test chamber was redesigned to permit high vacuum operation. In addition, the test chamber was provided with the necessary components to permit purging with inert gases. A new set of templin type grips was also manufactured for holding 1/4 inch diameter specimens at temperatures up to 3000^o F.

A more thorough redesign was necessary on the internal friction unit which was originally built for operation at a maximum temperature of approximately 1000^o C. The basic mode of excitation and detection remained the same as described earlier. However all components exposed to the high temperature environment as well as the heater and heat shields were replaced by columbium parts and the general configuration simplified to permit high vacuum sealing of all components in an all metal vacuum enclosure. This unit is now being assembled.

As pointed out in the discussion, grainsize was chosen as a primary experimental parameter. For this purpose a careful study was carried out

to establish a repeatable specimen preparation technique which did not suffer from introducing uncontrollable factors due to differences in heat treatment.

The material used for this study was the same as that used in the medium temperature work. The resulting techniques, after an unsuccessful try to establish a more economical approach, consisted of prestraining recrystallized specimens, both tantalum and columbium, to various percents of elongation, and subsequently, recrystallizing all specimens at the same temperature and for equal lengths of time. Figures 18a through 18d indicate the final grainsizes chosen for preliminary experiments. The specimens with larger grainsize were strained 15% prior to final recrystallization at 1300°C . In lieu of the availability of the high temperature internal friction unit, strain rate experiments were carried out with a limited number of available specimens. Strainrates of .005 inches/second and .00004 inches per second were utilized. The temperatures ranged from 500°F to 2900°F at 200°F intervals.

It was established that oxidation problems could be prevented with the system on hand up to the highest temperature. It was also definitely established that the strain rate sensitivity was very sensitive to grainsize over various portions of temperature range. For example, in the case of tantalum, the material with the larger grainsize was considerably more strain rate sensitive in the region from 1500°F to 1900°F and above 2600°F , than

was the material with the smaller grainsize. This trend was reversed near 500° F and near 2500° F. It is premature to present and evaluate these preliminary data in this technical report. The data have not as yet been verified as to their repeatability and are taken with experimental specimens which will not necessarily be identical to those being procured for the entire high temperature study. It is, however, intended to present the preliminary data in a forthcoming informal progress report (General Dynamics/Pomona M-349-1192).

Figure 18 TANTALUM – RECRYSTALLIZED AFTER 75% COLD REDUCTION



a. RECRYSTALLIZED ONLY (x 150)



b. 15% STRAIN & RECRYSTALLIZED (x 150)

COLUMBIUM – RECRYSTALLIZED AFTER 75% COLD REDUCTION



c. RECRYSTALLIZED ONLY (x 150)



d. 15% STRAIN & RECRYSTALLIZED (x 150)

SUMMARY & CONCLUSIONS

The shortcomings of theoretical models describing yield delay of body centered cubic metals purely on the basis of dislocation motion or purely on the basis of interstitial reorientation have been overcome by introducing the interstitial - dislocation interaction when a stress is applied.

The proposed theoretical model indicates that preyield microstrain is caused by interstitial reorientation during yield delay and that the time to yield is controlled by the ability of individual dislocation segments to leave their locking atmosphere. The latter mechanism, dislocation unpinning, is also controlled by the reorientation of interstitials into preferred positions. Consequently a similarity of activation energies for both processes is anticipated. The validity of the proposed theoretical model was primarily supported by the experimental results of mechanical yield delay experiments and by x-ray diffraction measurements of the crystal lattice behavior under load, prior to yield, and during recovery.

The yield delay experiments established that the effective activation energies measured from microstrain rate data and from time to yield data are approximately the same. The values range from approximately 8500 cal/mole to 14000 cal/mole between -97°F and 200°F , i.e., the range over which the most reliable data were obtained. This strongly indicates that hydrogen reorientation makes a major contribution to the yield delay mechanism. The variation in activation energies with temperature is explained in

terms of an effective activation energy resulting from multiple contributors to the anelastic behavior of bcc metals.

The stress dependence of the microstrain rate as well as of the time to yield was established theoretically as well as experimentally to be relatively temperature insensitive. This is in contrast to the theories which imply a significant reduction in activation energies by an activation volume concept, which can be expressed in terms of the exponential $\frac{Q-V\sigma}{RT}$. While the proposed model does not dispute the presence of a so-called activation volume term, it indicates its relative insignificance for the conditions investigated. A stress function of the form $\sigma e^{\beta\sigma}$ is introduced which is temperature independent, except for the fact that different stress ranges are by necessity employed in yield delay experiments at different temperatures and that β , similarly to the effective activation energies, is expected to vary with temperature due to contributions by different solutes.

It is shown that both the temperature variation of the activation energies and the temperature independence of the stress function have their analogy in macroscopic creep as was pointed out by the excellent results and accompanying survey by Professor Dorn⁽²²⁾.

The x-ray diffraction measurements showed quite clearly that reorientation of interstitials does take place during yield delay. Anelastic lattice deformations, following initial, elastic lattice strain, could be observed

and their full recovery established. It must be presumed that only interstitials can cause such anelastic lattice deformation. Slip of dislocation in isolated slip planes and even pile-ups occurring prior to yield cannot introduce a general, uniform lattice deformation; nor are dislocations, once formed likely to disappear and, thus, cause recovery of the lattice strain.

Mechanical yield delay recovery experiments yielded only qualitative information which indicated also that recovery of the yield delay mechanisms does take place but at considerably longer relaxation times. This is in agreement with the theoretical model which indicates the strong effects of an applied stress and is also in agreement with the x-ray diffraction measurements. Recovery information from the latter measurements is also only qualitative.

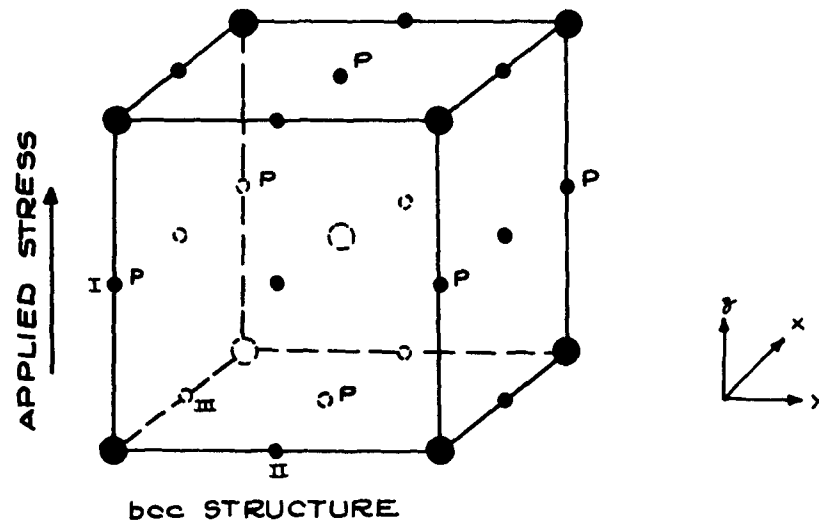
Internal friction measurements, though yielding satisfactory results with respect to agreement with other accepted values, did not contribute to the interpretation of the anelastic behavior of tantalum and columbium in the temperature ranges investigated in this phase of the contract. It was initially anticipated that oxygen, carbon and nitrogen would primarily contribute to the anelastic behavior as it did in other bcc metals. However it soon became apparent that hydrogen was the controlling interstitial. Due to the low activation energies of hydrogen diffusion, low temperature internal friction work would have been required. The available unit was not capable of this. The data obtained will be valuable for a

future phase of this contract.

This phase, a study of high temperature anelasticity of tantalum and columbium, was initiated with modification of equipment for operation up to 3000° F in a protective environment and with the development of sample preparation techniques for controlling grainsizes. Initial tensile experiments were performed on available specimens. These exploratory data are not presented in this report. Though interesting, they are as yet not reliably verified due to extremely limited sampling.

APPENDIX A

PRE-YIELD STRAIN AND STRESS INDUCED DIFFUSION IN BCC METALS



The pre-yield strain, ϵ_t , of a metal for a given load history, $\sigma = \sigma(t)$, may consist of a purely elastic term plus a diffusion induced strain, ϵ_d , at the time t . This can be expressed as

$$\epsilon_t = \frac{\sigma_t}{E_u} + \epsilon_d \quad (A1)$$

The unrelaxed modulus, E_u , is used here because it corresponds to the modulus observed when the strain rate is too high for significant diffusion to take place before yield is initiated. E_u is therefore indicative of the purely elastic strength of the metal under consideration.

\mathcal{E}_d should be proportional to

$$r_i \int_0^t (\dot{n}_p) dt$$

(A2)

where r_i is the radius of the interstitial atoms. \dot{n}_p is the number of interstitial atoms entering the preferred lattice positions per unit time.

From the theory of diffusion in solids, it is expected that diffusion of interstitial atoms is governed by Fick's laws, with the proper modifications for random walk phenomena.

By Fick's first law, the flow J of atoms per unit area normal to the flow and per unit time is given by

$$J = - D \frac{\partial n}{\partial x}$$

(A3)

where D is the diffusion coefficient and $\partial n / \partial x$ the concentration gradient. Also, Fick's second law introduces the time rate of change from

$$\frac{\partial n}{\partial t} = D \frac{\partial^2 n}{\partial x^2} \quad (A4)$$

For random walk in one direction, (say the x-direction) D_x is given by $\frac{1}{2} d^2 \bar{\Gamma}_x$, where d is the distance between neighboring interstitial positions and $\bar{\Gamma}_x$ the mean frequency of jumping in the x-direction.

In the unstressed bcc lattice there is equal probability for an interstitial to jump forward or backward in any one direction. From the figure, it may also be seen that one third of the interstitial atoms may jump in the x and y direction, one-third in the x and z direction, and one-third in the y and z direction. From these two observations, the average jump frequency can be expressed as

$$\bar{\Gamma}_x = \frac{1}{3} \left(\frac{1}{2} \right) \Gamma_{x_I} + \frac{1}{3} \left(\frac{1}{2} \right) \Gamma_{x_{II}} + \frac{1}{3} (0) \Gamma_{x_{III}} = \frac{1}{3} \Gamma_0$$

Since

$$\Gamma_{x_I} = \Gamma_{x_{II}} = \Gamma_{x_{III}} = \Gamma_0$$

Thus

$$D_x = \frac{1}{6} d^2 \Gamma_0 = \frac{1}{24} a^2 \Gamma_0 \quad (a = \text{lattice constant})$$

Now in the unstrained lattice

$$D_x = D_y = D_z = D \quad (A5)$$

The frequency Γ_0 with which an interstitial will jump into a neighboring position depends on the number of attempted jumps and the height of the barrier it has to overcome. This is illustrated in the final expression for the unidirectional diffusion coefficient⁽³⁰⁾.

$$D = \frac{1}{24} a^2 \nu \exp\left(\frac{\Delta S}{R} - \frac{Q}{RT}\right) \quad (A6)$$

where

- ν = frequency of atomic vibration
- Q = activation energy for interstitial diffusion
- R = gas constant
- T = absolute temperature
- ΔS = change in entropy

A good estimate of ν is given by $\nu = (2Q/a^2 m)^{1/2}$, where m is the mass of the interstitial atom. Also, to approximately evaluate the relation $\Delta S = -Q \cdot \partial(G/G_0) / \partial T$ may be used, where G_0 is the shear modulus at the reference temperature T_0 . Q itself can be evaluated experimentally to a fair degree of accuracy.

The concentration of interstitial atoms in all positions will vary with time. During a sufficiently small interval of time, Δt , the concentration of interstitial atoms, n_i , will always be large compared with

the fraction, Δn_i , leaving the respective positions, so that in the limit we may set $dn_i = -\lambda n_i dt$, λ being a proportionality or decay constant. Thus, at any time, t ,

$$n_i = n_0 e^{-\lambda t} \quad (A7)$$

We then find from Fick's second law

$$\begin{aligned} \frac{\partial n}{\partial x} &= \int_0^d -\frac{\lambda}{D} n_0 e^{-\lambda t} dx \\ &= -\frac{\lambda d}{D} n_0 e^{-\lambda t} \end{aligned} \quad (A8)$$

where d again is the distance between neighboring interstitial positions. Then

$$\left. \frac{\partial n}{\partial x} \right)_{t=0} = -\frac{\lambda d}{D} n_0 \quad (A9)$$

The assumption is now made that all nearest neighbor positions surrounding the interstitials are empty. This is reasonable for the usually low concentration of interstitials. Then the initial concentration gradient is simply $(-n_i/d)$. This results in a decay constant, defined by

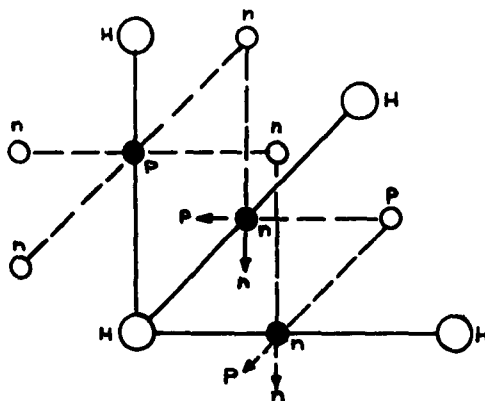
$$\frac{dn}{dt} = -\frac{D}{a^2} n_i = -\lambda n_i \quad (A10)$$

It must be noted that λ applies to unidirectional jump probabilities only. For the three dimensional case $\lambda = 4\Gamma$ in the unstrained lattice since there are four neighboring positions for each interstitial⁽³¹⁾.

The application of a stress, or better, the resulting lattice deformation, will create preferred and nonpreferred interstitial positions by a change in the local lattice energy. With respect to the diffusion equation this is accounted for by a variation in the activation energy. Normally, this change is considered proportional to the applied stress. We may then correct the activation energy for diffusion into the preferred position

$$Q_{n \rightarrow p} = Q - \ell \sigma, \text{ and, arbitrarily, for the reversed direction } Q_{p \rightarrow n} = Q + \ell' \sigma.$$

Considering the unit cell positions of interstitials in the strained bcc lattice, as shown in the figure below, we can treat the random walk process in terms of two unidirectional jump frequencies, one for atoms leaving the preferred positions and one for those entering.



Of the three basic positions one is preferred and all neighboring positions are nonpreferred. Two positions are nonpreferred, i.e. each contains one half of the interstitials in the nonpreferred positions, and only one half

of the attempts to leave are in the direction of a preferred neighboring position. This can be described as

$$\bar{\Gamma}_{p \rightarrow n} = 1(1) \Gamma_{p \rightarrow n}$$

$$\bar{\Gamma}_{n \rightarrow n} = \frac{1}{2} \left(\frac{1}{2} \right) \Gamma_{n \rightarrow p} + \frac{1}{2} \left(\frac{1}{2} \right) \Gamma_{n \rightarrow p} = \frac{1}{2} \Gamma_{n \rightarrow p} \quad (A11)$$

Consequently for unidirectional jump processes

$$\begin{aligned} D_{p \rightarrow n} &= \frac{1}{2} d^2 \Gamma_{p \rightarrow n} = \frac{1}{8} a^2 \Gamma_0 e^{-l\sigma/R\pi} \\ D_{n \rightarrow p} &= \frac{1}{4} d^2 \Gamma_{n \rightarrow p} = \frac{1}{16} a^2 \Gamma_0 e^{+l\sigma/R\pi} \end{aligned} \quad (A12)$$

Using the same notation as for the unstrained case, we note

$$\lambda_{n \rightarrow p} = \frac{1}{2} \Gamma_{n \rightarrow p} \quad \lambda_{p \rightarrow n} = \Gamma_{p \rightarrow n}$$

Now, to determine the net rate of interstitials jumping from the non-preferred into the preferred positions the following set of linear differential equations must be solved:

$$\left. \begin{aligned} \dot{n}_{p \rightarrow n} &= -\lambda_{p \rightarrow n} n_p + \lambda_{n \rightarrow p} n_n \\ \dot{n}_{n \rightarrow p} &= -\lambda_{n \rightarrow p} n_n + \lambda_{p \rightarrow n} n_p \end{aligned} \right\} \quad (A13)$$

This set has a solution

$$n_p = C_1 + C_2 e^{-(\lambda_n + \lambda_p)t} \quad (A14)$$

where

$$\lambda_n = \lambda_{n \rightarrow p} \quad \lambda_p = \lambda_{p \rightarrow n}$$

From the initial conditions

$$\dot{n}_p = -\lambda_p n_{p0} + \lambda_n n_{n0} \quad (t=0)$$

$$n_p = n_{p0} \quad (t=0)$$

we find

$$n_p = \frac{\lambda_n (n_{p0} + n_{n0})}{\lambda_n + \lambda_p} - \frac{\lambda_n n_{n0} - \lambda_p n_{p0}}{\lambda_n + \lambda_p} e^{-(\lambda_n + \lambda_p)t} \quad (A15)$$

and

$$\dot{n}_p = (\lambda_n n_{n0} - \lambda_p n_{p0}) e^{-(\lambda_n + \lambda_p)t} \quad (A16)$$

Equations (A15) and (A16) show the following expected features. The concentration of interstitials in the preferred position and therefore the anelastic strain reaches a finite or equilibrium value. Likewise, the strain rate approaches zero with time. In yield delay experiments this is not necessarily observed since the time to yield is relatively small.

From Equations (A10), (A11) and (A16) we can write

$$\begin{aligned} \dot{n}_p &= \left[\frac{1}{2} n_{n0} \Gamma_0 e^{l\sigma/RT} - n_{p0} \Gamma_0 e^{-l'\sigma/RT} \right] e^{-(\lambda_n + \lambda_p)t} \\ &= \frac{n_i}{3} \Gamma_0 \left[e^{l\sigma/RT} - e^{-l'\sigma/RT} \right] e^{-(\lambda_n + \lambda_p)t} \end{aligned}$$

since

$$n_i = n_{n0} + n_{p0} = \frac{2}{3} n_i + \frac{1}{3} n_i \quad (A17)$$

If the conditions $l \cong l'$ and $l\sigma \geq RT$ hold, we can utilize the approximation

$$\dot{\eta}_p = \frac{n_i}{3} \Gamma_0 e^{+\frac{l\sigma}{RT}} e^{-\lambda_n t} \quad (A18)$$

since λ_n is then also much larger than λ_p

Consequently the anelastic strain rate is given by

$$\dot{\epsilon}_d = C r_i n_i v e^{\Delta S/R} e^{-\left(\frac{Q-l\sigma}{RT}\right)} e^{-\lambda_n t} \quad (A19)$$

During yield delay experiments the exponent $\lambda_n t$ is initially very small and, as expected, a constant strain rate is observed during a portion of the experiment. It must be carefully considered in the data reduction that this is not true during the whole experiment unless the time to yield is small.

Thus, for the "initial" or linear portion of the strain rate we can utilize the following relations for data reduction.

$$\ln \dot{\epsilon} = A - (Q - l\sigma/RT) \quad (\sigma = \text{constant}) \quad (A20)$$

$$\ln \dot{\epsilon} = B + \frac{l}{RT} \sigma \quad (T = \text{constant}) \quad (A21)$$

Also, Equation (A15) can be approximated by

$$\begin{aligned}
 n_p &= n_i - n_{n0} e^{-\lambda n t} \\
 &= n_i \left[1 - \frac{2}{3} e^{-\lambda n t} \right] \\
 &= n_i \left[1 - \frac{2}{3} + \frac{2}{3} \lambda n t - \frac{2}{6} (\lambda n t)^2 + \dots \right]
 \end{aligned}
 \tag{A22}$$

or

$$n_p \cong \frac{n_i}{3} [1 + 2\lambda n t]$$

Thus $\dot{n}_p \cong \frac{2}{3} n_i \lambda n = \frac{1}{3} n_i \Gamma_0 e^{l\sigma/RT}$

which is the same result as (A18) for small value of $\lambda n t$.

Finally, Equation (A1) for arbitrary application of the load can be written:

$$E_t = \frac{\sigma(t)}{E_u} + K v_i n_i \int_0^t e^{-\frac{Q - l\sigma(t)}{RT}} e^{-\lambda n t} dt \tag{A23}$$

provided the conditions $l\sigma \geq RT$ and $l \cong l'$ are applicable.

Otherwise, Equation (A15) or (A16) must be introduced in (A1).

APPENDIX B

STRAIN OR STRESS INDUCED CHANGE IN THE ACTIVATION ENERGY OF INTERSTITIAL DIFFUSION

The effect of strain on the jump frequency for diffusion has been shown by Girifalco and Grimes⁽³²⁾ to be represented by the following expression:

$$\Gamma(\epsilon_{\alpha\beta}) = \Gamma_0 \exp \left\{ \frac{1}{kT} \sum_{\alpha,\beta} m_{\alpha\beta} \epsilon_{\alpha\beta} \right\} \quad (B1)$$

where $m_{\alpha\beta} = \left\langle \left(\frac{\partial \Phi}{\partial \epsilon_{\alpha\beta}} \right)_{q_{j,0}} \right\rangle_A - \left\langle \left(\frac{\partial \Phi}{\partial \epsilon_{\alpha\beta}} \right)_{q_{j,0}} \right\rangle_\sigma$

Γ_0 = jump frequency in absence of applied stress,

k = Boltzmann's constant T = absolute temperature, $\epsilon_{\alpha\beta}$ = strain tensor

and Φ_σ is the potential energy of the system with the diffusing atom at its activated position and Φ_A refers to the normal configuration. In order to obtain the statistical averages the potential energy is expanded in normal coordinates.

$$\Phi = \Phi(0) + \frac{1}{2} \sum_j \omega_j^2 q_j^2$$

where $\Phi(0)$ is the potential energy when all the atoms are at their mean positions for a particular strain, and ω_j and q_j represent natural frequencies and normal coordinates respectively. Now

$$\left(\frac{\partial \Phi}{\partial \epsilon} \right)_{\epsilon=0} = \left(\frac{\partial \Phi(0)}{\partial \epsilon} \right)_{\epsilon=0} + \sum_j \omega_j \frac{d\omega_j}{d\epsilon} q_j^2 \quad (B2)$$

It is at this point that we deviate from the derivation of Girifalco and Grimes. The term, $\left. \frac{\partial \phi(\omega)}{\partial \epsilon} \right)_{\epsilon=0}$, is not equal to zero since there is

an interaction of the particles of solute with the solvent. Otherwise there would be no lattice deformation associated with the presence of interstitials. Fastov⁽³³⁾ represents this interaction energy in a normal position as

$$C\psi_0 + l_1 C\epsilon_{ii} + l_2 (C_i \epsilon_{ii}) \quad (B3)$$

From this expression one can see that $\left. \frac{\partial \phi(\omega)}{\partial \epsilon_{\alpha\beta}} \right)_{\epsilon=0} = C_{xx} (l_1 + l_2 \delta_{xx}) \delta_{\alpha\beta}$

where C_{xx} is the number of solute atoms in the x position. In our case we can set $C_{xx} = 1$. Thus for the change in potential energy with strain we obtain

$$\left. \frac{\partial \phi}{\partial \epsilon_{\alpha\alpha}} \right)_0 = l_1 + l_2 \delta_{xx} - \sum_i \gamma_i \omega_i^2 g_i^2 \quad (B4)$$

for an interstitial in the x position in terms of a modified Grüneisen parameter

$$\gamma_i = - \frac{d \ln \omega_i}{d \epsilon_{\alpha\alpha}}$$

Substituting this expression into the equation for the statistical average

$$\left\langle \left. \frac{\partial \phi}{\partial \epsilon} \right)_0 \right\rangle = \frac{\int \dots \int \left. \frac{\partial \phi}{\partial \epsilon} \right)_0 e^{-\phi/kT} \pi dq_i}{\int \dots \int e^{-\phi/kT} \pi dq_i}$$

we obtain

$$\left\langle \left. \frac{\partial \phi}{\partial \epsilon_{xx}} \right)_0 \right\rangle = l_1 + l_2 \delta_{xx} - kT_i \sum \gamma_i \quad (B5)$$

l_1 and l_2 represent stress induced ordering parameters. Thus for the case of simple elastic tension we obtain for a preferred position

$$\frac{\Gamma}{\Gamma_0} = \exp \left\{ \frac{1}{kT} [(1-2\nu)l_1 + l_2] \varepsilon \right\} \exp \left\{ (1-2\nu) \sum_i (\gamma_i^A - \gamma_i^\sigma) \varepsilon \right\} \quad (B6)$$

where ν is Poisson's ratio, and, for a non-preferred position

$$\frac{\Gamma}{\Gamma_0} = \exp \left\{ \frac{1}{kT} [(1-2\nu)l_1 - \nu l_2] \varepsilon \right\} \exp \left\{ (1-2\nu) \sum_i (\gamma_i^A - \gamma_i^\sigma) \varepsilon \right\} \quad (B7)$$

The stress induced entropy of activation can be obtained from the relation

$$\Delta S = \frac{\partial}{\partial T} kT \ln \frac{\bar{z}_1}{\bar{z}_2}, \quad \text{where } \bar{z}_1 \text{ and } \bar{z}_2 \text{ are the partition}$$

functions of the activated and normal configuration. Thus

$$\Delta S = \frac{\partial}{\partial T} kT \left\{ \frac{1}{kT} [(1-2\nu)l_1 + l_2] \varepsilon + (1-2\nu) \sum_i (\gamma_i^A - \gamma_i^\sigma) \varepsilon \right\}$$

or

$$\Delta S = k(1-2\nu) \sum_i (\gamma_i^A - \gamma_i^\sigma) \varepsilon \quad (B8)$$

It is seen that the effect of strain on the lattice frequencies near a defect is also reflected in an entropy change. From the reciprocal temperature dependence of the interstitial relaxation strength observed in the Group V transition metals, ⁽²⁷⁾ one can conclude that the stress induced ordering parameter for interstitial diffusion is relatively temperature independent.

It is of interest to make a theoretical calculation of the activation energy and ordering parameter, Q , for an interstitial impurity in a typical bcc metal.

Although a theoretical calculation of the activation energy by a continuum elasticity theory ⁽³⁴⁾ gives fair agreement with experiment, the internal consistency of the large deformation correction is questionable. This calculation entirely neglects chemical valence effects. Actually the energy of activation is not just due to elastic strain, there is a non-elastic deformation. We will use a repulsive potential as Huntington did for fcc crystals. ⁽³⁵⁾ We will also include electrostatic interactions determined from a Thomas-Fermi model which considers the effect of electron redistribution on long range interactions.

Repulsive Energy - The Born-Mayer potential energy is of the form

$$V(r) = A \left(1 + \frac{Z_i}{n_i} + \frac{Z_j}{n_j} \right) e^{-\frac{r_i+r_j}{\rho}} e^{-\frac{r}{\rho}} \quad (B9)$$

where Z = valency of atom, n = number of electrons in outer closed shell. We will take ρ to agree with the early work of Born and Mayer, ⁽³⁶⁾

$\rho = .345 \text{ \AA}^0$. The radii of the ions will be taken to be $r(C^{++}) = .15 \text{ \AA}^0$ and $r(M_0^{++}) = .62 \text{ \AA}^0$. ⁽³⁷⁾

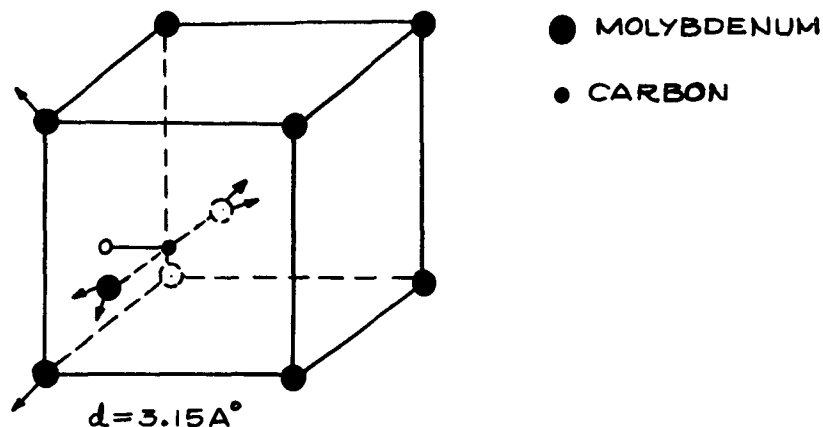
In order to determine the interaction constant in the Born-Mayer potential for a carbon atom and some other metallic atom we will minimize the repulsive energy with respect to local strain in the case of iron and select the value of the constant, b , which will give agreement with experiment.

The experimental value of local strain is 0.19, which was determined from martensitic tetragonality.⁽³⁸⁾ The repulsive energies are

$$\begin{aligned} (\text{Fe-C}) \quad E_i &= 344 a e^{-4.17(1+\xi)} \\ (\text{Fe-Fe}) \quad E_c &= 1110 e^{-4.17(2+(1+\xi)^2)^{\frac{1}{2}}} \end{aligned} \quad (\text{B10})$$

Parameters of the Fe-Fe and Mo-Mo repulsive interaction were determined from the calculated parameters of the Morse potential for cubic metals.⁽³⁹⁾ The resulting value of a is 0.15 for both metals.

The radial displacements considered are indicated in the figure.



We will calculate E_i , the interstitial interaction energy, for the hole position, by summing the two body interactions for an interstitial and two displaced host atoms. The energy of the complex, E_c , will be calculated by summing interactions for 2 displaced host atoms and 22 non-displaced host atoms.

$$\begin{aligned}
E_i &= 77 e \left\{ -4.57(1+\xi) \right\} \\
E_c &= 6260 e \left\{ -4.57(2+(1+\xi)^2)^{\frac{1}{2}} \right\} + 6260 e \left\{ -4.57(2+(1-\xi)^2)^{\frac{1}{2}} \right\} \quad (B11) \\
&\quad + 7820 e \left\{ -7.92 \right\}
\end{aligned}$$

where $\frac{\xi d}{2}$ is the displacement of nearest neighbor atoms.

The value of $\xi = 0.10$ was calculated by minimizing this repulsive energy. To calculate the energy of the barrier, we let E_i be the interaction energy of the interstitial and 4 displaced host atoms and E_c the interaction energy of 4 displaced host atoms and 20 non-displaced host atoms. Then

$$\begin{aligned}
E_i &= 154 \exp \left\{ -5.12(1+\delta) \right\} \\
E_c &= 6260 \exp \left\{ -4.57 \left[1 + \left(1 - \frac{\delta}{2}\right)^2 + (1-\delta)^2 \right]^{\frac{1}{2}} \right\} \\
&\quad + 3130 \exp \left\{ -7.92(1+\delta) \right\} + 6260 \exp \left\{ -4.57 \left[1 + \left(1 - \frac{\delta}{2}\right)^2 + (1+\delta)^2 \right]^{\frac{1}{2}} \right\} \\
&\quad + 6260 \exp \left\{ -4.57 \left[1 + \left(1 + \frac{\delta}{2}\right)^2 + (1-\delta)^2 \right]^{\frac{1}{2}} \right\} \quad (B12)
\end{aligned}$$

where $\delta d/2$ is the displacement of nearest neighbor atoms. From the minimization a value of $\delta = 0.05$ was calculated. The resulting values of energy are

$$E(\text{hole})_R = 7.89 \text{ eV.}$$

$$E(\text{barrier})_R = 8.60 \text{ eV.}$$

Electrostatic Energy - In order to consider electrostatic interactions we shall only consider interactions with 6 host atoms and 8 host atoms in the hole and barrier position, respectively. This is possible because the interaction is screened by conduction electrons.

Lasarus' result for the potential is

$$\phi(r) = \frac{ze}{r} \exp(-qr) \quad (B13)$$

where $q^2 = \frac{4me^2}{\hbar^2} \left(\frac{3N_0}{\pi} \right)^{1/3} = 1.65,$

and z is the valence difference, and N_0 is the conduction electronic density, taken to be 1 electron/atom for Mo. Lasarus' original theory (40) was applicable to substitutional impurities. In an interstitial solution we are not merely replacing regular atoms and thus we are interested in the total potential energy of an impurity atom. Since the valence charge of carbon is +4 the sign of electrostatic interaction represents repulsion. The charge of the molybdenum atom which the screened carbon atom interacts with will be taken to be +6. Although the 4d electrons do not fill a band, their effective mass is large (small band width) and they are thus localized. (41)

Actually the number of free electrons to be used in determining the screening constant is not determined simply by the electron arrangement in the outer s and d atomic levels. It is known from band theory that the d and s bands overlap and, as a result, there are deviations from the simple picture, there always being less than one s electron per atom in the transition elements. (42)

More accurate solutions (40) of the Thomas-Fermi equation for repulsive electronic forces gives a potential of the form

$$\phi(r) = \frac{ze\alpha(z)}{r} \exp(-qr) \quad (B14)$$

for tightly bound electrons. The potential energy of carbon in molybdenum is

$$V = \frac{173}{r} \exp -2.23r$$

for $\alpha = 0.5$. Thus

$$E(\text{hole})_E = \frac{173(2)}{1.58(1+\xi)} e^{\left\{-2.61(1+\xi)\right\}} + \frac{173(4)}{2.24} e^{\left\{-3.7\right\}} = 18.88 \text{ ev.} \quad (\text{B15})$$

and

$$E(\text{barrier})_E = \frac{173(4)}{177(1+\delta)} e^{\left\{-2.06\left[(1+\delta)^2 + \left(1+\frac{\delta}{2}\right)^2\right]^{\frac{1}{2}}\right\}} + \frac{173(4)}{2.84} e^{\left\{-4.7\right\}} = 19.56 \text{ ev.} \quad (\text{B16})$$

Therefore, $E(\text{hole}) = 26.77 \text{ ev.}$ and $E(\text{barrier}) = 28.16 \text{ ev.}$ From the difference in barrier energy and the energy of the interstitials in the equilibrium position, the activation energy for diffusion is calculated to be 32,000 cal/mole for molybdenum. This value is in reasonable agreement with the experimental value ranging from 25,000 to 33,400 cal/mole. ^(8, 24)

In order to calculate the stress induced ordering parameter Q we must calculate $\partial E / \partial \sigma$ at the barrier position and a non-preferred hole position. In terms of small elastic strain, the energy expressions are given by the following:

$$\begin{aligned} E(\text{hole}) = & 77 e^{\left\{-4.57(1.1)(1-\nu E)\right\}} + 6260 e^{\left\{-8.2(-.66\nu E)\right\}} \\ & + 6260 e^{\left\{-7.66(1+.36E-.64\nu E)\right\}} + 7820 e^{\left\{-7.92\left(1+\frac{1}{3}E-\frac{2}{3}\nu E\right)\right\}} \\ & + \frac{173(2)}{1.58(1.1)} e^{\left\{-2.61(1.1)(1-\nu E)\right\}} + \frac{173(4)}{2.24} e^{\left\{-3.7\left(1+\frac{E}{2}-\frac{\nu}{2}E\right)\right\}} \quad (\text{B17}) \end{aligned}$$

$$\begin{aligned}
E(\text{barrier}) = & 77 e \left\{ -5.12(1.05) \left(1 + \frac{\epsilon}{2} - \frac{\nu \epsilon}{2} \right) \right\} + 77 e \left\{ -5.12(1.05)(1 - \nu \epsilon) \right\} \\
& + 313 e \left\{ -4.57(1.93 - 1.96 \nu \epsilon + .9) \right\} + 313 e \left\{ -4.057(1.93 - 1.86 \nu \epsilon + \epsilon) \right\} \\
& + 3130 e \left\{ -7.92(1.05) \left(1 + \frac{\epsilon}{3} - \frac{2}{3} \nu \epsilon \right) \right\} + 3130 e \left\{ -4.57(2.03 - 1.96 \nu \epsilon + 1.1 \epsilon) \right\} \\
& + 3130 e \left\{ -4.57(2.03 + \epsilon - 2.06 \nu \epsilon) \right\} \\
& + 3130 e \left\{ -4.57(1.98 + .9 \epsilon - 2.06 \nu \epsilon) \right\} + \frac{173(2)}{1.77(1.05)} e \left\{ -3.02(1 + .51 \epsilon - .49 \nu \epsilon) \right\} \\
& + \frac{173(2)}{1.77(1.05)} e \left\{ -3.02(1 - \nu \epsilon) \right\} - \frac{173(2)}{2.84} e \left\{ -4.7 \left(1 + \frac{\epsilon}{2} - \frac{\nu \epsilon}{2} \right) \right\} \\
& + \frac{173(2)}{2.84} e \left\{ -4.7(1 - \nu \epsilon) \right\} + 3130 e \left\{ -4.57(1.98 + \epsilon - 1.96 \nu \epsilon) \right\} \quad (B18)
\end{aligned}$$

We neglected the variation with strain in $\frac{1}{V}$ as compared to $e(-qr)$.

From the above expressions and using ν = Poisson's ratio = 0.32 we calculated the following derivatives:

$$\left. \frac{\partial E}{\partial \sigma} (\text{hole}) \right|_{\epsilon=0} = -3.3 \times 10^{-3} \frac{\text{Cal.}}{\text{mole-psi}} \quad (B19)$$

$$\left. \frac{\partial E}{\partial \sigma} (\text{barrier}) \right|_{\epsilon=0} = -2.8 \times 10^{-3} \frac{\text{Cal.}}{\text{mole-psi}} \quad (B20)$$

These results indicate that while there is an effect of stress on the energy of the interstitial in the equilibrium position there is a negligible

effect on the activation energy for diffusion of interstitials (in this example carbon in molybdenum). This is because the energy of the non-preferred hole is lowered by a comparable amount to the barrier energy.

Due to the lack of appropriate data a similar analysis for H in Ta and Cb was not carried out at this time. However it is possible to obtain a reasonable estimate of the stress induced ordering parameter for interstitial diffusion in the metals being considered from the variation in solid solution lattice spacing with concentration of solute atoms in a martensitic lattice.⁽⁴³⁾ The uniform variation with concentration of hydrogen interstitials has been measured for Ta and Cb⁽⁴⁴⁾. Fisher has derived an expression for the change in lattice spacing with concentration in the uniform and the martensitic state.⁽³⁸⁾ From these expressions one can derive the result

$$\frac{\partial \epsilon}{\partial \rho} \text{ (martensitic)} = \frac{9}{2(1-2\nu)} \frac{\partial \epsilon}{\partial h} \text{ (uniform)} \quad (\text{B21})$$

where $\rho = r_z - \eta/3$ represents the ordering parameter.

Using these results we calculate values of .017 cal/mole-psi for hydrogen in Ta, and .022 cal/mole/psi for H in columbium. The value obtained for columbium agrees very well with the dependency of the activation energy on stress observed from the yield point by Wilcox et al.⁽¹⁸⁾

APPENDIX C

EFFECT OF THE STRESS FIELD OF DISLOCATIONS ON INTERSTITIAL DIFFUSION

The effect of diffusion of the dilute Snoek atmosphere on the flow stress of iron has been previously considered.⁽⁴⁵⁾ Also there is expected to be an effect of reorientation of the Cottrell atmosphere, due to dislocation assisted jumps, on the upper yield stress. In addition to diffusive motion the impurity atoms acquire a steady drift velocity given by $(D_I/RT) F$, where F is the interaction force provided by a dislocation. Mura et al.⁽²⁰⁾ calculated the force on the locking atoms to be given by a linear function of stress. It is felt that the direct effect of dislocation bulging on the interstitial jump frequency Γ_I should also be taken into account. It is necessary to review the theory of dislocation-interstitial interactions in order to obtain a clear picture of the bound interstitial sites. The dislocation and interstitial sites being considered are indicated in Figure C1.

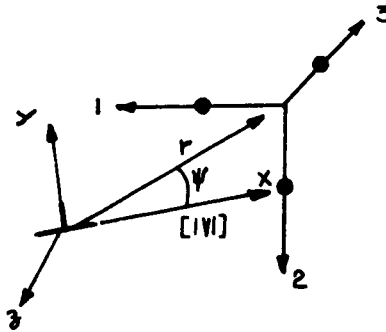


FIGURE C1

The following expression for the interaction energy has been derived
by Cochardt et al. ⁽⁴⁶⁾

$$U_{DC} = \frac{Da^3}{r} \left\{ \begin{aligned} &\frac{1}{3} \sin \psi (1 + \nu + 2 \cos^2 \psi) (\epsilon_1 + \epsilon_2 + \epsilon_3) \\ &-\frac{1}{2} \sin \psi \cos 2\psi (\epsilon_2 + \epsilon_3) \\ &-\frac{\sqrt{6}}{3} \cos \psi \cos 2\psi (\epsilon_3 - \epsilon_2) + \nu \sin \psi \epsilon_1 \end{aligned} \right\} \quad (C1)$$

where $D = \frac{Gb}{2\pi(1-\nu)}$ and $\epsilon_1, \epsilon_2, \epsilon_3$ represent the martensitic strains along the crystal axes. It turns out that interstitials on axes 2 and 3 have a wide minimum in energy below the slip plane ($\psi = \frac{3}{2}\pi$) and, also, interstitials on axis 2 have a sharp minimum on the slip plane ($\psi = 0$).

From this result we conclude that atoms below the slip plane provide most of the locking because there are a larger number of preferred sites below slip plane and also that atoms in the slip plane attract dislocations in the slip direction. A shift of impurity atoms from below the slip plane to the slip plane will reduce the locking force and also pull the dislocation further along the slip plane. Our picture of the jump process is indicated in Figure C2.

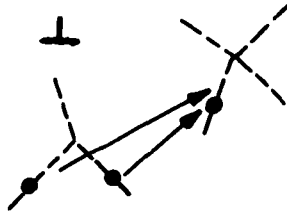


FIGURE C2

We will now calculate the effect of a stress induced dislocation displacement upon the interstitial binding energy at sites below and on the slip plane. We refer to Figure C3 for the definition of x, y and x_0 .

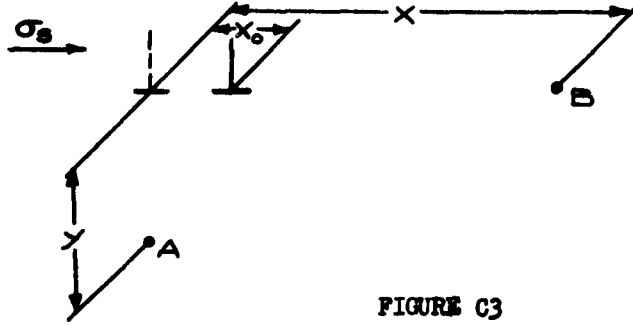


FIGURE C3

Position A refers to the unit cell with origin at the matrix atom below the slip plane. Position B refers to the unit cell with origin at the matrix atom in the slip plane. The interaction energy below the slip plane simplifies to

$$V = -\frac{A \sin \theta}{r} = -\frac{Ay}{x_0^2 + y^2} \quad (C2)$$

Equating the force $\sigma_s b^2$, applied on a dislocation segment of length b , to the locking force we obtain

$$x_0 = \frac{\sigma_s b^2 y^3}{2An} \quad (C3)$$

where n is the number of locking atoms. The energies at cells A and B

become
$$V_B = -\frac{A}{x-x_0} = -\frac{A}{x} - \frac{A}{x} \left(\frac{x_0}{x} \right) + \dots$$

$$V_A = -\frac{A \sin \theta}{r} = -\frac{A}{y} + \frac{A}{y} \left(\frac{x_0^2}{y^2} \right) + \dots \quad (C4)$$

For small dislocation displacements (keeping only terms linear in $\frac{x_0}{x}$ and $\frac{x_0}{y}$) we obtain

$$V_A - V_B = - \frac{\Delta x_0}{x^2} = - \frac{\Delta y^3 b^2 \sigma_s}{2 \Delta x^2 n} \quad (C5)$$

The averages of x and y are set equal to $R/2$, where R is the radius of the atmosphere. This radius has been defined previously by Cottrell as $R = A/kT$ (47). Schoeck and Seeger (45) also confirm the applicability of this definition.

The number of locking atoms, n , is given by $\pi R^2 b^2 C_I a^{-3}$, where C_I is the atomic concentration of interstitials. We will assume that C_I is the same as the concentration of the lattice interstitials. In columbium, as used in this study, the atomic concentration, C_I , is 2.8×10^{-4} and this corresponds to an atmosphere of 1 atom per atomic length of dislocation within the radius R .

Thus

$$\Delta V = - \frac{A b^2 R a^3 \sigma_s}{8 \pi A b R^2 C_I} = - \frac{b a^3 \sigma_s k T}{8 \pi C_I A} \quad (C6)$$

and

$$\frac{\Delta V}{kT} = - \frac{b a^3 \sigma_s}{8 \pi C_I A} \quad (C7)$$

The microstrain rate resulting from Equation (C7) will behave as

$$\dot{\epsilon} = K \sigma \exp \left\{ - \frac{Q}{RT} + \beta \sigma \right\} \quad (C8)$$

As an estimate of A , we will take the value $1.5 \times 10^{-20} \text{ dyne-cm}^2$, found for the interaction between carbon interstitials and dislocations in iron. ⁽⁴⁷⁾

Using our expression for β as defined by Equation (C7) we calculate values of $3.3 \times 10^{-4} (\text{psi})^{-1}$, $1.6 \times 10^{-4} (\text{psi})^{-1}$ in columbium and tantalum respectively. The expression for β involves the impurity concentration, C_I , and the interaction constant A . It can be used to evaluate the product $A C_I$ but not either factor separately. Thus it is possible that the interaction constant, A , is smaller and the concentrations C_I , greater than the values used.

It is essential to consider an atmosphere continuously distributed within a radius $R = A/kT$ in order to obtain an energy change that is linearly dependent on temperature. Likewise the impurity atmosphere has been represented by Beshers in terms of a continuous Fermi-Dirac distribution. ⁽⁴⁸⁾

APPENDIX D

MAGNITUDE OF ANELASTIC STRAIN NORMAL TO THE APPLIED STRESS

The anelastic strain will be determined from a thermodynamic derivation following Brinkman and Schwarzl,⁽⁴⁹⁾ except that we will consider the 3-dimensional case. For an equilibrium condition

$$\rho = C(\epsilon, T) \exp \left[- \frac{V(q) + v(\epsilon, q)}{kT} \right], \quad \int \rho dq = n \quad (D1)$$

where ρ = density, ϵ = strain, T = temperature, q = position coordinate, k = Boltzmann's constant, V = potential energy due to lattice, v = potential energy change due to stress.

At equilibrium states, the entropy and internal energy are given by

$$S = -k \int_{-\infty}^{\infty} \rho \log \rho dq + S_{\text{elastic}}$$

$$U = \int_{-\infty}^{\infty} (V + v) \rho dq + U_{\text{elastic}} \quad (D2)$$

Now, taking a differential change in ϵ

$$T \delta S = \delta U + \sigma \delta \epsilon$$

Then

$$T \frac{\partial S_{\text{elas.}}}{\partial \epsilon_i} \delta \epsilon_i = \int \rho \frac{\partial v}{\partial \epsilon_i} dq \delta \epsilon_i + \frac{\partial U_{\text{elas.}}}{\partial \epsilon_i} \delta \epsilon_i$$

$$+ \int (V + v) \frac{\partial \rho}{\partial \epsilon_i} dq \delta \epsilon_i + \sigma_i \delta \epsilon_i \quad (D3)$$

$i = 1, 2, 3$

and upon using

$$\int \frac{\partial P}{\partial \epsilon_i} dq = 0$$

we get

$$\sigma = \frac{E v \epsilon_1}{1-v-2v^2} + \frac{E v \epsilon_2}{1-v-2v^2} + \frac{E(1-v)\epsilon_3}{1-v-2v^2} - \ln n_1; \quad l = \frac{\partial v}{\partial \epsilon}$$

$$0 = \frac{E v \epsilon_1}{1-v-2v^2} + \frac{E v \epsilon_2}{1-v-2v^2} + \frac{E(1-v)\epsilon_3}{1-v-2v^2} - \ln n_2$$

$$0 = \frac{E v \epsilon_1}{1-v-2v^2} + \frac{E v \epsilon_2}{1-v-2v^2} + \frac{E(1-v)\epsilon_3}{1-v-2v^2} - \ln n_3 \quad (14)$$

$$\text{or } E \epsilon_1 = \sigma + \ln n_1 - 2v \ln n_2$$

$$\begin{aligned} E \epsilon_2 = E \epsilon_3 &= \ln n_2 (1-v-2v^2) - v(\sigma + \ln n_1 - 2v \ln n_2) \\ &= -v\sigma - v \ln n_1 + \ln n_2 (1-v). \end{aligned} \quad (15)$$

Thus the ratio of transverse to longitudinal anelastic strain is given by

$$\begin{aligned} \frac{\varepsilon_2}{\varepsilon_1} &= \frac{\ln_2(1-\nu) - \nu \ln_1}{\ln_1 - 2\nu \ln_2} \\ &= -\nu \frac{\ln_1 - \ln_2 \left(\frac{1-\nu}{\nu} \right)}{\ln_1 - 2\nu \ln_2} \end{aligned} \quad (D6)$$

and since $2\nu < \frac{1-\nu}{\nu}$ for $\nu < 0.5$

the transverse strain is always smaller than indicated by Poisson's ratio.

APPENDIX E

ACTIVATION ENERGIES DEFINING THE YIELD DELAY TIME AND THE MICROSTRAIN RATE

From Equations (13) it is seen that

$$Q'_{eff} = R \frac{d \ln t_y}{d(\frac{1}{T})} \quad (E1)$$

and, likewise,

$$Q''_{eff} = -R \frac{d \ln \dot{\epsilon}}{d(\frac{1}{T})} \quad (E2)$$

Thus $Q'_{eff} = \frac{1}{t_y} \frac{d}{d(\frac{1}{T})} \left\{ \lambda_I^{-1} (1 - e^{-\lambda_I t_y}) - \lambda_D^{-1} \right\}$ (E3)

where

$$C = \frac{\ln N_{D_0}}{N_{D_0} - N_{Cr}}$$

This leads to

$$\begin{aligned} Q'_{eff} &= \frac{1}{t_y} \left[Q_I \lambda_I^{-1} (1 - e^{-\lambda_I t_y}) \lambda_I^{-1} e^{-\lambda_I t_y} (Q_I \lambda_I t_y - \lambda_I t_y Q'_{eff}) \right. \\ &\quad \left. + Q_D \lambda_D^{-1} C \right] \\ &= Q_I (\lambda_I t_y)^{-1} + \left[Q_D C (\lambda_D t_y)^{-1} - Q_I e^{-\lambda_I t_y} \right] (1 - e^{-\lambda_I t_y})^{-1} \end{aligned}$$

which can be simplified by introducing Equation (10) to

$$Q'_{eff} = \frac{Q_I - Q_D}{\lambda_I t_y} + \frac{Q_D - Q_I e^{-\lambda_I t_y}}{1 - e^{-\lambda_I t_y}} \quad (E4)$$

For very small values of t_y , or better $\lambda_I t_y$, this leads to

$$Q'_{eff} \cong Q_I$$

The activation energy of the strain rate has a somewhat simpler form.

Rewriting Equation (12) in the form

$$\dot{\epsilon} = C' \lambda_I e^{-\lambda_I t} \quad (E5)$$

we have, on using the same definition of λ_I as above,

$$\begin{aligned} Q''_{eff} &= - \frac{R d \ln \dot{\epsilon}}{d(\frac{1}{T})} \\ &= - \frac{R d}{d(\frac{1}{T})} \left[\ln C' + \ln A - \frac{Q_I}{RT} - A t e^{-\frac{Q_I}{RT}} \right] \\ &= Q_I - t Q_I A e^{-\frac{Q_I}{RT}} \end{aligned}$$

$$\text{or } Q''_{eff} = Q_I (1 - \lambda_I t) \quad (E6)$$

REFERENCES

- 1) Vreeland, Wood & Clark, Transactions of the American Society of Metals 45, 620 (1953).
- 2) Hendrickson, Wood & Clark, Transactions of the American Society of Metals 48, 540 (1956).
- 3) Fisher, Transactions of the American Society of Metals 47, 451 (1955).
- 4) Vreeland and Wood, Eighth Technical Report under Office of Naval Research, California Institute of Technology (April 1954).
- 5) Cottrell, Reported at Conference on High Rates of Strain, Institute of Mechanical Engineers, (April, 1957).
- 6) Mura and Brittain, Acta Metallurgica 8, 767 (1960).
- 7) Peiffer, Acta Metallurgica 9, 385 (1961).
- 8) Sneed and Kornblum, Convair/Pomona TM 332-127, 15 (1958).
- 9) Davidenko, Smirnov and Yaroshevich, Soviet Physics - Solid State 3, 1254 (1961).
- 10) Adams and Iannucci, Aeronautical Systems Division Technical Report 61-203, (1961).
- 11) Adams, Roberts and Smallman, Acta Metallurgica 8, 328 (1960); Johnson, Acta Metallurgica 8, 737 (1960).
- 12) Chambers and Schultz, Physical Review Letters 6, 273 (1961); Bordoni, Nuovo & Verdini, Physical Review 123, 1204 (1961); Chambers, Bulletin of the American Physical Society 6, 521 (1961).
- 13) Conrad and Schoeck, Acta Metallurgica 8, 791 (1960).
- 14) Palm, Metallen 3, 97, 120 (1949).
- 15) Louat, Proceedings of the Physical Society 71, 444 (1958).
- 16) Bennett and Sinclair, University of Illinois T. & A.M. Report 157, (1959).
- 17) Weinstein, Sinclair and Wert, University of Illinois T. & A.M. Report 156, (1959).

- 18) Wilcox, Brisbane and Klinger, WADD Technical Report 61-44, (1961).
- 19) Roshanskii & Stepanova, Soviet Physics - Doklady 5, 831 (1961).
- 20) Mura, Tamura and Brittain, Journal of Applied Physics 32, 92 (1961).
- 21) Seeger, Donth and Pfaff, Discussions of the Faraday Society 23, 19 (1957); Niblett and Wilks, Advances in Physics 9, 17 (1960).
- 22) Dorn, Creep and Recovery, 277 (1957).
- 23) Albrecht, Goode and Mallett, Journal of the Electrochemical Society 106, 981 (1959).
- 24) Samsonov and Latysheva, Doklady, Nauk S.S.S.R. 109, 582 (1956); Samsonov and Latysheva, Fix Metal i Metalloved 2, 309 (1956).
- 25) Samsonov and Solonnikova, Physics of Metals and Metallography 5, 177 (1957).
- 26) Peterson, Wright Air Development Division Technical Report 60-793, (1961).
- 27) Powers and Doyle, Journal of Applied Physics 30, 514 (1959).
- 28) Wert and Marx, Acta Metallurgica 1, 113 (1953).
- 29) Zener, Elasticity and Anelasticity of Metals, 68 (1948).
- 30) LeClaire, Progress in Metal Physics 4, 265 (1953).
- 31) Zener, Imperfections in Nearly Perfect Crystals, 289 (1952).
- 32) Girifalco and Grimes, Physical Review 121, 982 (1961).
- 33) Fastov, Soviet Physics, Doklady 6, 431 (1961).
- 34) Ferro, Journal of Applied Physics 28, 895 (1957).
- 35) Huntington, Physical Review 91, 1092 (1953).
- 36) Seitz, Modern Theory of Solids, 82 (1940).
- 37) Kittel, Introduction to Solid State Physics, 82 (1956).

- 38) Fisher, Acta Metallurgica 6, 13 (1958).
- 39) Girifalco and Weiser, Physical Review 114, 687 (1959).
- 40) Lazarus, Solid State Physics (Ed. Seitz and Turnbull) 10, 98 (1960).
- 41) Dekker, Solid State Physics, 61, 68 (1957).
- 42) Sinnott, The Solid State for Engineers, 117, 402 (1958); Herring, Journal of Applied Physics, Supplement to 31, 38 (1960).
- 43) Nowick, Progress in Metal Physics 4, 35 (1953).
- 44) Pearson, A Handbook of Lattice Spacings and Structures of Metals and Alloys 4, 972, 977 (1958).
- 45) Schoeck and Seeger, Acta Metallurgica 7, 469 (1959).
- 46) Cochardt, Schoeck and Wiedersich, Acta Metallurgica 3, 533 (1955).
- 47) Cottrell, Dislocations and Plastic Flow in Crystals, 136 (1953).
- 48) Beshers, Acta Met. 6, 521 (1958); Kamber, Keefer and Wert, Acta Metallurgica 9, 403 (1961).
- 49) Brinkman and Schwarzl, Discussions of the Faraday Society 23, 11 (1957).